INSTITUTE OF PLASMA PHYSICS

NAGOYA UNIVERSITY

WORKSHOP ON RELATION BETWEEN

LABORATORY AND SPACE PLASMAS

IPPJ-286 May 1977

RESEARCH REPORT

NAGOYA, JAPAN

WORKSHOP ON RELATION BETWEEN LABORATORY AND SPACE PLASMAS

IPPJ-286 May 1977

Further communication about this report is to be sent to the Research Information Center, Institute of Plasma Physics, Nagoya University, Nagoya, Japan.

WORKSHOP ON RELATION BETWEEN LABORATORY AND SPACE PLASMAS

FORWARD

The idea to hold a workshop on relation between laboratory and space plasmas originated early in 1975 as a natural outcome from joint investigations performed between laboratory and space plasma physicists. Their backgrounds are, to some extent, quite different with a resulting difference in terminology and language and frequently in point of view, but a mutual communication between them is in fact possible through a common language in terms of basic plasma physics. Further, there is a growing tendency that new research, i.e. frontier research is becoming interdisciplinary, multidisciplinary. It was, therefore, felt that an exchange of information would be useful and profitable to seek out new interdisciplinary problems to link both areas.

Institute of Plasma Physics, Nagoya University adoped this idea with a suggestion that a series of workshop might be suitable to discuss specific topics and to cover a wide range of comparison between laboratory and space plasmas.

Along this line, the first workshop was held on May 28 - 29, 1976 and focused the problem to the topic of "Charged-Particle Beams in the Laboratory and Space" in view of a growing interest in the problems of solar-terrestrial relationship and controlled electron-beam experiments in space, for instance by means of a "Space Shuttle-Spacelab".

The new aspect of this workshop is a remarkable blending of laboratory and space plasmas. The organizers have thus attemped to arrange a marriage between laboratory or fusion and space physicists. From the papers given

at the workshop, it may be stated that while the marriage is agreed upon on both sides, it will perhaps be postponed to the next meeting. We hope, however, this workshop will add some new and interesting ingredients.

This report endeavors to convey the progress of the meeting, presenting all lectures in a printed but limited form.

H. Kikuchi

A. Miyahara

H. Obayashi

TABLE OF CONTENTS

INTRODUCTION - PLASMAS IN THE LABORATORY AND SPACE

H. KIKUCHI

Nihon University, College of Science and Technology, Tokyo and
Nagoya University, Institute of Plasma Physics, Nagoya, Japan

A number of laboratory experiments performed for the study of plasma of thermonuclear interest has been found to have a correspondence to important basic phenomena observed in space and astrophysics.

First of all, one finds that energetic processes taking place on the sun itself can be regarded as a "pattern" of controlled nuclear fusion. Our human dream in the 20th century is to simulate these solar processes on the Earth on a "breadboard scale", thus realizing a nuclear fusion reactor for terrestrial projects, e.g. for the development of new energy sources.

Another example is a basic phenomenon involving the conversion of magnetic energy into plasma kinetic energy in the laboratory and space which is currently being studied with the so-called "multipole devices" in the laboratory. These machines are characterized by metallic conductors immersed in a plasma and carry the currents producing the confining magnetic fields. In space, this phenomenon occurs in relation to the field line merging or reconnection in the neutral sheet of the Earth's magnetotail or the solar prominences.

Table 1 shows a correspondence between laboratory and space plasmas, based upon model machines furnished at Institute of Plasma Physics, Nagoya University. On the laboratory side, current efforts are being directed to the understanding of the processes of plasma heating, turbulence, and slowing down of fast electron, ion and neutral beams by using toroidal and other devices that have been developed for the confinement of high temperature

TABLE 1. CORRESPONDENCE IN LABORATORY AND SPACE PLASMAS

(based on experimental devices)

Laboratory	Space
Torus (Stellarator, Tokamak, Zeta)	Solar atmosphere or corona, Hot gaseous nebula, Hot interstellar gas
TPD II & III (IPPJ) : Multi-cusp devices (Surmac)	Cusp, Neutral-point or -line (Earth)
Multi-pole devices (Inverse pinch)	Neutral sheet - X-type field line merging or reconnection (Earth's magnetotail, Solar prominences)
Multi-dipole devices (Surmac)	Neutral sheet (Solar prominences)
CCT-I & II (IPPJ) : Caulked-cusp torus machines	O-type field line merging or reconnection (Earth's magnetotail, Solar prominences)
BSG II (IPPJ) : MACH II (IPPJ) (Turbulent heating devices)	Turbulence in the plasma trough or high-latitude auroral zone and in the solar corona or interplanetary space (Earth, Solar flares)
TPH-II (IPPJ) (Electron cyclotron resonant heating & electron beam injection)	Ionospheric heating
REB & ERA (Cerenkov, Cyclotron or Synchrotron radiation)	Solar bursts, Pulsars
Space chamber (Quiescent plasma) : DP (IPPJ) : TPC (IPPJ) (Shocks, Solitons)	Plasmasphere, Plasmapause

plasmas. These processes are found to have a direct relevance to solar flare phenomena involving the onset of strong plasma turbulence and to the formulation of X-ray star models.

Table 2 shows plasma structure and instabilities in singular regions in solar-terrestrial plasmas which play crusial roles in a variety of solar-terrestrial phenomena. The term "zeroth order" indicates spatial steady thermal structure typically represented by the plasmasphere or the plasmapause in the Earth's magnetosphere. Plasma irregularities or ducts with some maintenance period can be regarded as the zeroth order plasma structure. The "first or higher order" plasma structure indicates temporal plasma structure or variations, plasma fluctuations or instabilities which are essentially plasma waves or turbulence. According to our study, for instance, the Earth's plasmapause is thought to be a manifestation of a kind of electrostatic shocks caused by the intersection of a super-ion-sonic convective flow with the terrestrial plasma and exhibits large plasma density discontinuities but no zeroth order magnetic field discontinuities. The universal instability for the first or higher order plasma

TABLE 2. SINGULAR REGIONS IN SOLAR-TERRESTRIAL PLASMAS

Region	0th order structure (Spatial structure)	1st or higher order (Temporal) structure	Instability	Energy, Temperature (°K)	Plasma density (cm-3)	Laboratory simulation or plasma
Photosphere	Origin of black body radiation	Visible light and infrared emission	Thermodynamic equilibrium	10^4	10^{12}	
Sunspot	Origin of magnetic fields at low and middle latitudes	Periodic growth & decay	Flute or Rayleigh-Taylor, Interchange	5×10^3		Plasma coaxial accelerator
Plage & Flare	Origin of H_α, C_aII, X etc.	Optical, H_α, Proton, Cosmic, X ray emission Type III, IV bursts Explosive interplanetary wind	Tearing mode, Rayleigh-Taylor, Kink	10^7	10^{11}	Plasma coaxial accelerator Electron beam - plasma interaction
Chromosphere & Spacules	Relatively cold plasma	Hot plasma jet	Universal, Kink	10^5	10^6 10^{12}	
Prominence	Neutral sheet	Flare-associated explosive wind	Two stream; Kelvin-Helmholtz,			Multi-pole or dipole devices, Multi-cusp devices
Corona	Fully ionized hot plasma	Solar wind origin	Universal, Kink	10^6	10^6	
Magnetopause (Bow shock, Magnetosheath)	MHD shock (turbulent)	MHD or Alfvén wave	Kelvin-Helmholtz, Two stream	50eV	10	Terrella exp. Collisionless shock
Plasmapause	Electrostatic shock (laminar)	Drift wave	Universal	eV	10^2	Electrostatic shock & soliton
Proton ring current	Earthward edge of plasma sheet proton	Alfvén wave (Pc-1)	Cyclotron, Mirror	50eV	1	Curved & gradient drift exp.
Inner edge of plasma sheet	Solar or polar wind origin	Alfvén wave (Pi-1) + micro. turbulence	Universal	keV	0.25	Collisionless shock
Trapping boundary of radiation belt	Outer edge of radiation belt	Cyclotron wave	Flute, Cyclotron Universal	MeV ~50keV	10^{-4}	Mirror devices
Neutral sheet	current sheet	O- & X-type reconnection	Tearing mode	keV	1	Multi-pole or dipole devices
Polar cusp (Neutral point or line)	Entry of magnetosheath plasma	Alfvén & whistler wave, Electrostatic wave (whistler & micropulsation)	Kelvin-Helmholtz, Two stream, Universal	eV-keV	1~10	Multi-cusp devices (Surmac), Coaxial plasma resonator
Polar cap	Auroral oval	Auroral breakup VLF-ELF emission	Universal, Kink, Two stream	eV-keV	$1\sim10^5$	Terrella exp.
Ionosphere	Terrestrial origin (UV ionization)	E- & F-layer irregularities	$\underline{E} \times \underline{B}$, Two stream, Parametric	eV	10^5	Space chamber, Plasma production devices

structure is a source mechanism of the electrostatic waves or turbulence which can easily be converted into hydromagnetic waves due to plasma inhomogeneities or irregularities, as seen in geomagnetic pulsations.

In discussing laboratory simulation of space phenomena, it is most convenient to use the similarity laws based upon invariance of the nondimensional quantities of the Vlasov equation. Table 3 shows the Vlasov scaling laws for some basic physical quantities with numerical examples of scales between space and laboratory experiments. The invariablity of elementary particle properties makes potentials, temperatures, energies and velocities invariant. This means that lengths and times must obey the same scaling ratio. The scaling of any other physical quantity can easily be deduced from Table 3.

Because of the limitations arising from ideal similarity requirements indicated in Table 3, no real scaling of astrophysical phenomena down to

TABLE 3. VLASOV SCALING LAWS

Scaling laws	Solar chromosphere → Laboratory	Magnetosphere → Laboratory	Unit
L	$10^{6} \rightarrow 1$	$10^{7} \rightarrow 1$	m
$t \sim L$			
$B \sim L^{-1}$	$10^{2} \rightarrow 10^{8}$	$10^{-4} \rightarrow 10^{3}$	gauss
$N \sim L^{-2}$	$10^{14} \rightarrow 10^{26}$	$10^{6} \rightarrow 10^{20}$	m^{-3}
$E \sim L^{-1}$	$10^{-4} \rightarrow 10^{2}$	$10^{-5} \rightarrow 10^{2}$	V/m
$V \sim L^{0}$	$10^{5} \rightarrow 10^{5}$	$10^{5} \rightarrow 10^{5}$	m/sec
Energy $\sim L^{0}$			
Potential $\sim L^{0}$			

laboratory size is possible in general because of a large number of involved parameters which obey different scaling laws.

However, there is a wide class of astrophysical phenomena in which basic physical processes are important rather than geometry. In this case, laboratory simulation plays a crucial role in understanding basic processes involved in astrophysical phenomena.

Confining the first topic of a series of workshop to the problem of "Charged-Particle Beams in the Laboratory and Space", there are two classes of current interest in electron beams. One is concerned with relativistic high current beams from the point of view of thermonuclear interest on the laboratory side. Another interest is in controlled electron-beam experiments in space, for instance by means of a "Space Shuttle-Spacelab".

The experiments on beam-plasma interactions are of great varieties and spread over a wide range of areas. In general they are sorted into two kinds, linear and nonlinear. When high current beams are injected into a plasma, nonlinear interactions will be expected in a variety of forms such as shocks, solitons, harmonic generations, Čerenkov and cyclotron radiation, parametric interactions or plasma turbulence resulting in strong plasma heating.

Specifically in space, the injection of electron or ion beams into the plasmasphere has generated "artificial auroras", electrostatic plasma waves or resonances (EPR, ECH, LHR), triggered emissions, VLF waves, as observed by the Aerobee rockets, a series of "ECHOS". These "ECHOS" have also observed "electron echos" with a couple of bounces between the northern and southern hemispheres.

Very recently, there has been a number of proposals for feasibilities of a "Space Shuttle-Spacelab" for this kind of controlled electron beam experiments, in connection with the emergence of a new type of spacecraft, "Space Shuttle" that is being planned by NASA in 1980s.[1] In this connection, the problem of vehicle charge neutralization is becoming severe particularly for the case of a space shuttle, because more and more areas are being covered with non-conducting materials.

With regard to solar phenomena related to electron beams, significant are direct observations of type III radio bursts by the solar probe "HELIOS" which reached the perihelion of 0.3 AU closer to the sun than the innerst planet Mercury. These observations have demonstrated the generation mechanism of type III bursts through a two-step process that was originally proposed in 1958.

Going back to the discussions held at the present workshop, it can be stated that the scope of topics includes many aspects and roles of charged particle beams and covers a nearly whole range of areas in space and the laboratory. Although each paper itself may not link the laboratory and space necessarily, there can be found, from the plasma physics point of view, fairly close connections between one and another paper that would be helpful for a link between laboratory and space.

References

1. For instance, see ABSTRACTS of "Symposium on Active Experiments in Space Plasmas", Boulder, Colorado, June,1976.

Plasma Waves Observed By Sounding Rockets

I. Kimura

(Dept. of Electrical Eng., Kyoto Univ. Kyoto 606)

1. Introduction

Several rockets have been launched at Kagoshima Space Center(KSC), Kyushu, Japan and at Syowa Base, Antarctica, aiming at observation of plasma wave phenomena spontaneously or artificially occuring in the ionospheric plasma. In this report some interesting results will be introduced, with a view to having valuable comments on our results from other plasma physicists, in reference to the wave phenomena observable in the laboratory plasma.

2. Plasma phenomena associated with low energy electron beam[1),2),3)]

In the K-9M-41 rocket experiment performed on January 17, 1973, VLF plasma waves were observed in association with the ejection of an electron beam of a few eV. The electron beam of several tens of μA was emitted from a hot cathode through a potential sink of the rocket body, when a positive dc bias changing from 0 to 10 V at a 1 V step each second, was applied to a receiving dipole antenna(10m tip to tip) in order to increase the pick up factor of the antenna by removing an ion sheath around the antenna. Configulation of the antenna, dc bias and hot cathode is sketched in Fig. 1.

On the VLF plasma wave, the following results were obtained.

Case I The step dc bias was applied but the hot cathode was not turned on: By the dc bias over 3 volts, the pick up factor of the dipole antenna was outstandingly improved, and LHR like continuous emissions were observed as well as many whistlers.

Case II The step dc bias was applied and the hot cathode was turned on; In addition to the usual whistlers and the other LHR like emissions, discrete emissions with a frequency spectrum resembling the shape of the letter 'U' was observed for the dc bias over 3 eV, as shown in Fig. 2. The U emissions appeared twice per spin period of the rocket, nearly 1 second. The emission frequency was always lower than the local LHR frequency, and the minimum frequency of each U spectrum decreased with increasing dc bias, or energy of the electron beam.

In order to interpret the above characteristics of U-emissions we have postulated that the instantaneous frequency of the emissions depends on the energy of the beam. By a careful examination, we have found that the frequency of each U shape, which varied synchronously with the rocket spinning, decreases with increasing energy component of the beam in the direction of the geomagnetic field.

Although the energy of the electron beam in the direction of the magnetic field is found to be associated with the frequency of the emissions, it is rather difficult to interpret them by a simple instability theory, because 1) the frequency is less than the local LHR frequency, 2) the emission was not affected by the Doppler effect due to rocket velocity, so that the phase velocity of the wave should be much larger than the rocket velocity of the order of 1 km/s.

An interaction between an electron beam and ion Bernstein modes, has been investigated, but in that case the emissions should appear at all harmonics of the ion cyclotron frequency. An interaction of the electron beam with a whistler mode wave propagating in the direction nearly perpendicular to the geo-

magnetic field, has also been examined. However, any instability by which whistler mode waves are amplified only at frequencies below the LHR frequency, has not been found.

3. Rocket experiment at Syowa Base.

In this experiment which was made on February 13, 1976 at Syowa Base, Antarctica, plasma waves in the VLF range were observed by a loop and dipole antenna. Throughout the rocket flight, whistler mode VLF emissions, so called 'chorus'[4] in the frequency range from 0.2 to 0.8 kHz, and discrete noises in the frequency above 1 kHz were observed. The former was simultaneously observed on the ground. The latter was only observed by mainly the dipole antenna of the rocket (partly by the loop antenna of the rocket), and the intensity and frequency were strongly modulated by the rocket spin motion, being very similar to the U shaped emission previously introduced. An example of sonagram containing these emissions is shown in Fig. 3. In the present case, however, no hot cathode was installed. The dc bias was intermittently applied to the dipole antenna, but the emission was observed whether the dc bias was on or not. At the time of rocket flight, no aurora existed, so that abundant particle precipitation, which could be a kind of beam, was not expected to exist, although the data of the rocket borne particle analyser are now under analysis.

At present, we postulate that such emissions may be produced just in the vicinity of the rocket, due to a kind of wake effect. The mode of the wave can be the ion acoustic wave.

4. Conclusion

I have introduced two rocket experiments, in which a kind

of plasma wave that may be produced in the vicinity of the rocket, was observed. These phenomena depend or do not depend on the electron beam in the space. We are interested in a relation between these waves and those appearing in laboratory plasmas.

Finally, I appreciate the discussion made at my presentation of this report on May 28, 1976 at the Institute of Plasma Physics, Nagoya University.

References

1) H. Matsumoto, S. Miyatake and I. Kimura, Frequency spectra of VLF plasma waves observed by Japanese ionospheric sounding rocket K-9M-41. Rept. Ionosph. Space Res. Japan, 28, 89, 1974

2) H. Matsumoto, S. Miyatake and I. Kimura, Rocket experiment on spontaneously and artificially stimulated VLF plasma waves in the ionosphere, J. Geophys. Res., 80, 2829, 1975

3) H. Matsumoto, I. Kimura, S. Miytatake and T. Obayashi, Active sounding rocket experiment, using ~3eV electron beams, on wave-particle interaction, Space Res. XVI, 601, Akademic-Verlag, Berlin 1976.

4) R. A. Helliwell, Whistlers and related ionospheric phenomena, Stanford Press, 1964.

Figure captions

Fig. 1 Configulation of the dipole antenna, dc bias circuit and hot cathode(F_1-F_2) for the K-9m-41 rocket.

Fig. 2 Plasma phenomena observed by the K-9M-41 rocket; whistlers, LHR emissions and U shaped emissions(A and B).

Fig. 3 Chorus($f < 0.8$ kHz) and U shaped emissions($f > 2$ kHz) observed by an antarctic rocket, S-310JA-1.

Fig. 1

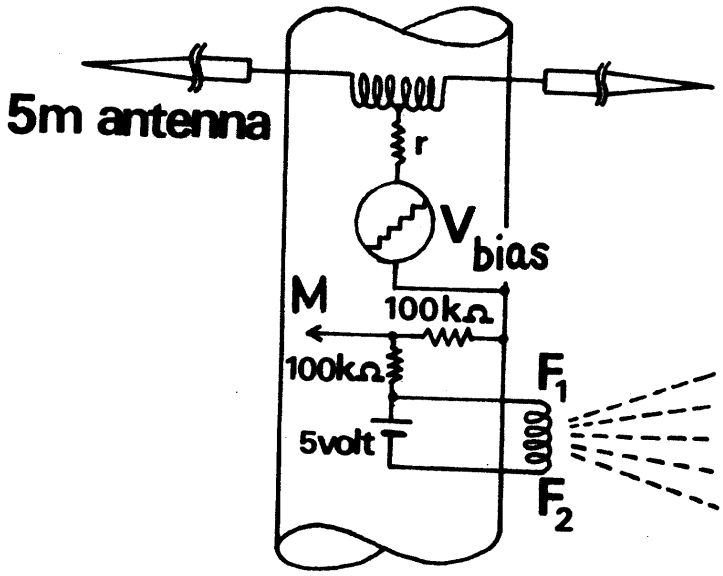

Fig. 2

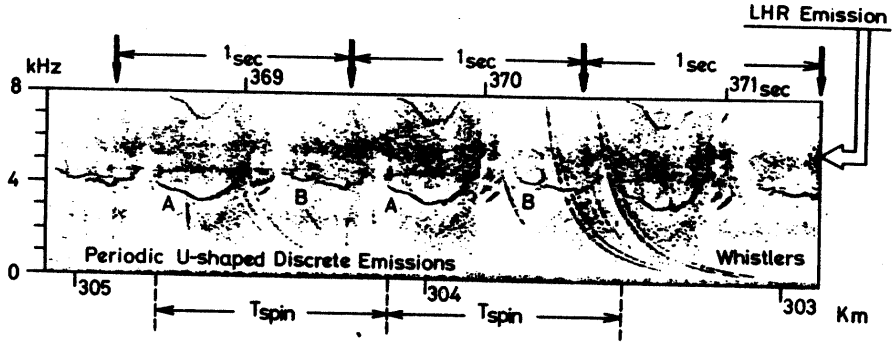

Fig. 3

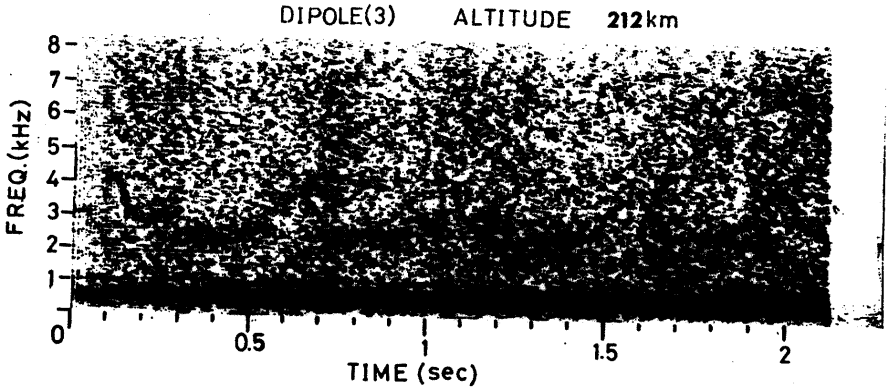

Feedback Stabilization of Drift-Cyclotron Instability and its Application to Space Plasma

Yoshihiro Higuchi

Department of Electrical Engineering

Yamagata University

Yonezawa Japan

1. Introduction

The drift-cyclotron instabilities may occur when the drift wave mode associated with the density gradient intersects ion cyclotron modes in the dispersion diagram. The stabilization methods for the drift-cyclotron instabilities have been proposed by several authors; shear stabilization, finite beta stabilization, the stabilization by means of externally applied high frequency electric and magnetic field and feedback stabilization.

The purpose of this note is to show the possibility of the drift-cyclotron instability on the boundary of the so-called polar cusp and to discuss on the possibility of the stabilization by the feedback control method.

2. Density Feedback Control (4) (5)

Consider an inhomogeneous plasma in which the density gradient is in the x-direction. The plasma is located in a constant magnetic field which is in the z-direction. The application of feedback system is as follows: the output signal sensed by Langmuir probe is phase shifted, amplified and added back into the imput signal. In order to obtain the dispersion relation Vlasov equation with the feedback source term and the Poisson equation are used. In addition, the feedback source term is assumed to be proportional to the local density perturbation. The local dispersion relation becomes

$$K^2 = -\sum_{j=e,i} \frac{k_{dj}^2 \left\{ 1 + \frac{(\omega - \omega_j^*)}{k_z v_j} \sum_{n=-\infty}^{+\infty} Z(\zeta_j)\, e^{-b_j} I_n(b_j) \right\}}{1 + \frac{\omega_{fj}}{k_z v_j} \sum_{n=-\infty}^{+\infty} Z(\zeta_j)\, e^{-b_j} I_n(b_j)},$$

where $k_{dj}^2 = (4\pi n_0 e^2)/T_j$, $\omega_j^* = k k_y T_j / m_j \omega_{cj}$, $k = \frac{\partial \ln n_0}{\partial x}$,

$b_j = k_y^2 T_j / m_j \omega_{cj}^2$, $\zeta_j = (\omega - n\omega_{cj})/k_z v_j$, $Z(\zeta_j) = \frac{1}{\sqrt{\pi}} \int_{-\infty}^{+\infty} \frac{e^{-x^2} dx}{x - \zeta_j}$.

$I_n(b_j)$ is the modified Bessel function with order n. The amplitude and argument of $i\omega_{fj}$ represent the gain and phase of the feedback system, respectively.

In order to obtain the simplified dispersion relation for flute mode the several assumptions will be made. When $\omega \approx n\omega_{ci} \ll \omega_{ce}$, only the $n = 0$ term of the summation is retained for electron. However, all terms need to be kept for ion. Suppose the condition of the long

wavelength for electron($b_e \ll 1$) where the component of the wavelength perpendicular to the magnetic field is much greater than the mean cyclotron radius of the electron, then $I_0(b_e)\, e^{-b_e} \approx 1 - b_e$.
On the other hand, suppose the condition of short wavelength for ion ($b_i \gg 1$) where the component of the wavelength perpendicular to the constant magnetic field is much shorter than the mean cyclotron radius of the ion, then $\sum_n I_n(b_i) e^{-b_i} \approx (2\pi b_i)^{-1/2}$. The asymptotic expansion of the plasma dispersion function can be used for both the ion and the electron under the condition of $k_z v_j < (\omega - n\omega_{cj})$. The electron temperature is assumed to be zero. Making all the above assumptions, the simplified dispersion relation for the flute mode may be obtained as

$$1 + \frac{k_i^2}{k_\perp^2} + \left(\frac{\omega_{pe}}{\omega_{ce}}\right)^2 \frac{\omega}{\omega - \omega_{fe}} - \frac{k_i^2}{k_\perp^2} \frac{\omega_i^*}{\omega - \omega_{fe}} = \frac{k_i^2}{k_\perp^2} \frac{1}{\sqrt{2\pi b_i}} \sum_{n=-\infty}^{+\infty} \frac{\omega - \omega_i^*}{\omega - n\omega_{ci}} ,$$

Stability Analysis; the drift wave frequency with the density feedback effect is written as

$$\omega_1 \equiv \frac{\omega_i^* + \omega_{fe}(1 + k_\perp^2 \lambda_{di}^2)}{1 + k_\perp^2 \lambda_{di}^2 (1 + \frac{\omega_{pe}^2}{\omega_{ce}^2})} .$$

By the application of the density feedback the intersections between the drift wave mode and the ion cyclotron wave mode can be removed, if the following condition is satisfied,

$$k^2 \rho_i^2 < 4\pi^2 \left(\frac{V_A^2}{c^2} + \frac{m_e}{m_i}\right) + 4\pi \left\{2\left(\frac{\lambda_{di}}{\rho_i}\right)^2 + \frac{V_A^2}{c^2} + \frac{m_e}{m_i}\right\}\left(\frac{\omega_{fe}}{\omega_{ci}}\right) + 8\left(\frac{\lambda_{di}}{\rho_i}\right)^2 \left(\frac{\omega_{fe}}{\omega_{ci}}\right)^2$$

where $\rho_i = v_i/\omega_{ci}$, $\lambda_{di} = k_i^{-1}$, $n = 1, 2, 3, \ldots$, and V_A is the Alfven wave velocity.

3. Potential Feedback Control(6)

In this section the another type of feedback stabilization will be briefly discussed. The local potential perturbation may be taken as the control variable. The total potential ϕ_T in the plasma is different from the perturbation potential ϕ without potential feedback, such as $\phi_T = \phi + F\phi_T$, $\phi_T = \frac{1}{1-F}\phi = \underset{\sim}{K}\phi$, where the absolute value of F represents the feedback gain. The frequency independent potential feedback with 180° phase shift will be assumed, that is, F is real and negative so that $\underset{\sim}{K} < 1$. Then, the simplified dispersion relation for the flute mode may be written as

$$1 + \frac{\underset{\sim}{K}}{k_\perp^2 \lambda_{di}^2}\left\{ 1 + k_\perp^2 \lambda_{di}^2 \left(\frac{\omega_{pe}}{\omega_{ce}}\right)^2 - \left(\frac{\omega_i^*}{\omega}\right) - \frac{1}{\sqrt{2\pi b_i}} \sum_{n=-\infty}^{+\infty} \frac{\omega - \omega_i^*}{\omega - n\omega_{ci}} \right\} = 0,$$

Stability Analysis; The drift wave frequency with the potential feedback effect is written as

$$\omega_2 = \frac{\omega_i^*}{1 + k_\perp^2 \lambda_{di}^2 \left(\frac{1}{\underset{\sim}{K}} + \frac{\omega_{pe}^2}{\omega_{ce}^2} \right)} .$$

The points of intersections of the two branches, ω_2 and $n\omega_{ci}$, can be removed by the application of the potential feedback, if the following condition is satisfied

$$1 < \frac{c^2}{V_A^2}\left\{ \left(\frac{k\rho_i}{2n}\right)^2 - \frac{m_e}{m_i} \right\} < \frac{1}{\underset{\sim}{K}} .$$

$(n = 1, 2, 3, \cdots)$

4. Possibility of Drift-Cyclotron Instability on the Boundary of the Polar Cusp (1)(2)(3)

The interaction between the solar wind plasma and the geomagnetic field produces two neutral regions on the noon-midnight meridian, one in the northern hemisphere and one in the southern hemishere. The neutral region has been termed as polar cusp or cleft. From poleward of the cusp the geomagnetic field lines are swept back into the geomagnetic tail. The possible direct penetration of solar wind plasma through the polar cusp into the polar ionosphere has been inferred. The boundary of the polar cusp is a particularly interesting region because of the great variety of plasma instabilities that are excited there. One of the plausible plasma instabilities may be the drift-cyclotron instability on the boundary of the polar cusp. Unfortunately, the exact density gradient on the boundary is unknown. According to the satellite observation, the characteristic length of the density gradient could be less than 14 km. For the other plasma parameters on the boundary, the ion thermal velocity and ion cyclotron frequency are assumed as 10^{6} cm/sec, 10 rad/sec, respectively. The Debye wave number could be 10^{-3} cm^{-1}. Thus, the nondimensional diamagnetic drift velocity $\tilde{V}_{dn}$ $(= \frac{k_i V_{dn}}{\omega_{ci}})$ is about 10. The instability growth rates of the drift-cyclotron instabilities on the boundary of the polar cusp are shown in Fig. 1.

The application of the feedback stabilization discussed in the previous section will be made. For the density feedback control the dispersion relations obtained by numerical computation are shown in Fig. 2. In the absence of the feedback($\tilde{\omega}_{fe} = 0$) there are two unstable regions, but, in the presence of the feedback($\tilde{\omega}_{fe} = 2$) there is no intersections between the two branches. For the potential feedback control the dispersion relations are shown in Fig. 3.

References

(1) Higuchi,Y., Canad.J.Phys. 52, 1265, 1974

(2) Higuchi,Y., Nature(Phys. Sci.) 246, 117, 1973

(3) Higuchi,Y., IAGA(Kyoto) Bulletin No.34, 379, 1974

(4) Kitao,K., Plasma Physics. 13, 667, 1971

(5) Kitao,K., J.Phys.Soc.Japan, 35, 272, 1973

(6) Kitao,K., Nucl. Fusion in press

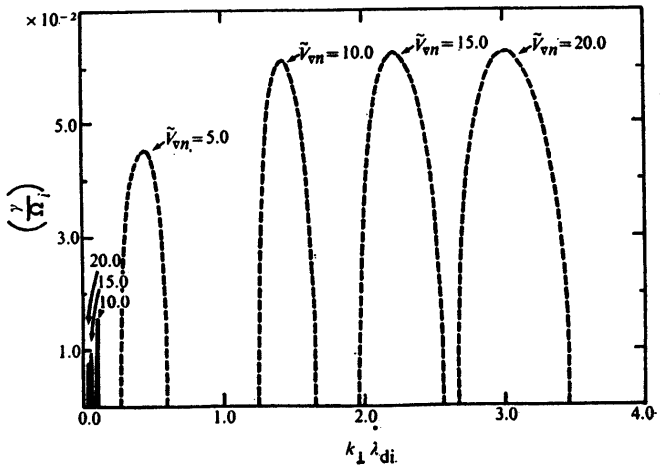

Fig. 1

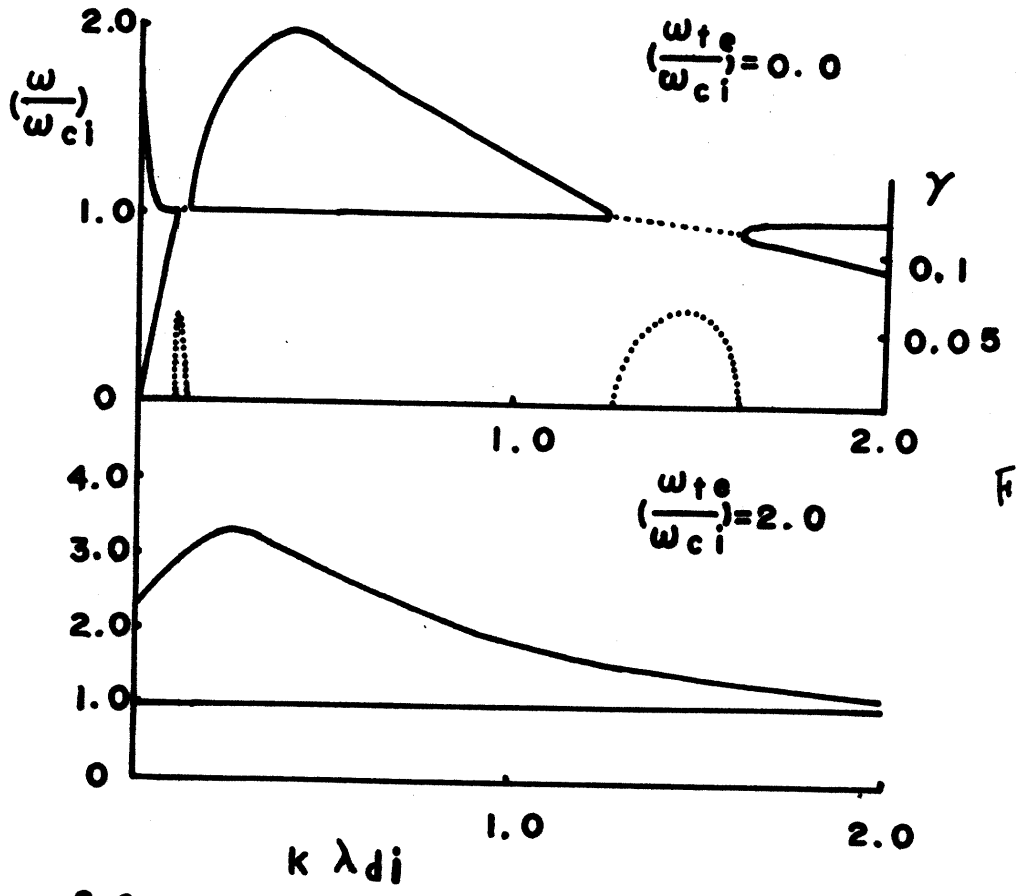
2.0
$(\frac{\omega}{\omega_{ci}})$
1.0
0
$(\frac{\omega_{te}}{\omega_{ci}})=0.0$
γ
0.1
0.05
1.0
2.0
4.0
3.0
2.0
1.0
0
$(\frac{\omega_{te}}{\omega_{ci}})=2.0$
1.0
2.0
$k\lambda_{di}$

Fig. 2

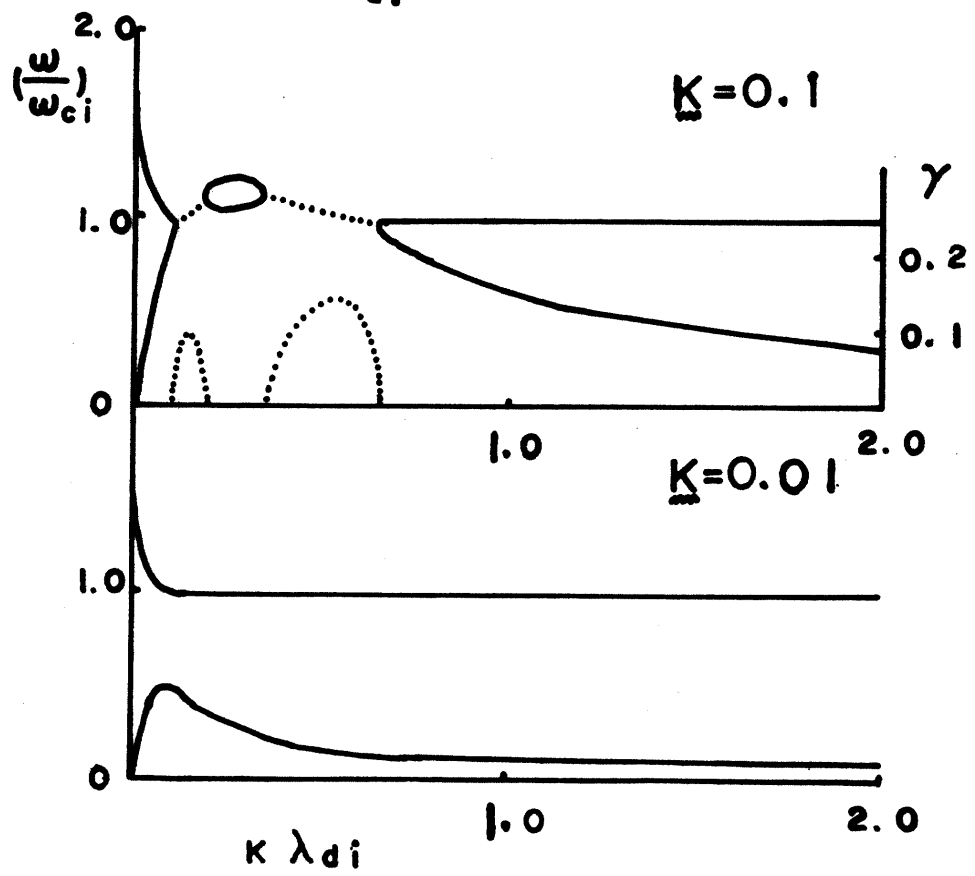
2.0
$(\frac{\omega}{\omega_{ci}})$
$K=0.1$
1.0
0
γ
0.2
0.1
1.0
2.0
$K=0.01$
1.0
0
1.0
2.0
$k\lambda_{di}$

Fig. 3

Propagation and Expansion of an Electron Beam Ejected from the Space Shuttle into the Ionosphere

Y.Kiwamoto
Research Institute for Energy Materials,
Yokohama National University

From 1980, a large scale orbiter [space shuttle] will start flying around the earth with various kinds of large instruments on board. Active plasma experiments on the shuttle are expected to explore a new field in plasma physics. One of the most attractive experiments is the study of the interaction between the high current electron beam and the ionospheric plasma. Unfortunately our knowledge of the macroscopic behavior of the electron beam is still in its infancy, although it is indispensable to set out requirements for various plasma detectors. The purpose of this article is to provide a simple model for depicting the macroscopic behavior of the electron beam propagating into the ionospheric plasma.

An analysis is made separately in two regimes, the collisionless regime [$t \ll 10$ msec] and the collisonal regime [$t \gtrsim 10$ msec]. In the collisionless regime the orbit of a test electron initially at the beam periphery is analyzed. After the expansion stops in this regime, a slow expansion takes place through collisions with neutral particles. This process is analyzed in terms of diffusion across the magnetic field.

(a) Collisionless Regime

If we neglect the reaction of the ambient plasma, the beam column expands due to the radial electric field caused by the

excess charge of the beam itself. In cylindrical co-ordinate frame (r,ϕ) moving with the beam with velocity u, the equations of motion of the test electron are

$$\ddot{r} - r\dot{\phi}^2 = \frac{e}{m} E + r\omega_c\dot{\phi} \quad , \tag{1}$$

$$r\ddot{\phi} + 2\dot{r}\dot{\phi} = -\omega_c\dot{r} \quad . \tag{2}$$

We impose the initial conditions as $(r,\phi)=(a_0,0)$, $(\dot{r},\dot{\phi})=(v,0)$. The electron field eE/m is related to the initial beam density n_0 as $eE/m=2\pi n_0 e^2 a_0^{\,2}/mr=\alpha^2/r$. Notations are conventional. For simplicity the magnetic field B is assumed to be constant. Equations (1), (2) integrate to

$$\frac{1}{2}\dot{\xi}^2 + U(\xi) = \frac{1}{2}\left(\frac{v}{a_0}\right)^2 \quad . \tag{3}$$

$$U(\xi) = \frac{\omega_c^2}{8\xi^2}(\xi^2 - 1)^2 - \left(\frac{\alpha}{a_0}\right)^2 \ln\xi \quad . \tag{4}$$

Here r is normalized as $\xi=r/a_0$. The effective potential $U(\xi)$ is schematically shown in Fig.1. The test particle oscillates in the region $0 < \xi \leq \xi_c$. After the test particle turns back from $\xi=\xi_c$ inward, another electrons arrive at $\xi=\xi_c$ and the beam radius remains around $\xi=\xi_c$ or $r=a_0\xi_c$. For our present interest $\xi_c^{\,2}>>1$, and we obtain the relation

$$\xi_c = 2\frac{\omega_b}{\omega_c}\left\{\ln\xi_c + \left(\frac{v}{u}\right)^2 \frac{u^2}{a_0^{\,2}\omega_b^{\,2}}\right\}^{1/2} \quad , \tag{5}$$

where $\omega_b^{\,2}=4\pi n_0 e^2/m$. The initial beam divergence θ is defined

by $\tan\theta=v/u$.

If an electron beam is injected into the ionosphere with initial paratmeters $E_b=mu^2/2=10keV$, $I_b=\pi a_0^2 en_0 u=2A$, $a_0=21.8cm$, $n_0=10^6 cm^{-3}$, $a_0\xi_c$ is determined by the divergence θ and the magnetic field strength which we assume B=0.3 gauss here. The relation between θ and $a_0\xi_c$ is plotted in Fig.2. In the case of $\theta=0$ and $(\omega_c/2\omega_b)^2 \leq 10^{-3}$, ξ_c is expressed as

$$\xi_c \approx 1.41\left(\frac{\omega_c}{2\omega_b}\right)^{-1.1} . \qquad (6)$$

This means that the average beam density $\bar{n}_b$ reaches a constant value determined mainly by B : when B=0.3 gauss, $\bar{n}_b=2\times10^3 cm^{-3}$. Integration of eqs. (3), (4) indicates that the beam radius increases from a_0 to $a_0\xi_c$ in a time of order $\tau_1=\pi/\omega_c\approx0.5\mu sec$.

(b) Neutralization of the Beam Charge

When the beam energy E_b is sufficiently high, the reactive motions of the ambient plasma is transverse to the beam. Because the electron Larmor radius is small, the reaction of the ambient electrons is not effective if some collective motions perpendicular to the magnetic field do not work. The ambient ions with temperature T_i and density n_i neutralize the excess charge in a time of $\tau_2 \lesssim (n_0/n_i)(a_0/\xi)(m_i/T_i)^{1/2} \sim 20\mu sec$. This value sets an upper limit to the neutralization time.

(c) Collisional Regime

The collision frequency with neutral atoms is the largest one for high energy beam electrons, being $\sim10^2 Hz$. In the time scale of 10^{-2}sec, the electric field does not exist and the diffusion transverse to the magnetic field occurs. The diffusion

coefficient $D_\perp$ across the magnetic field is approximately

$$D_\perp = 1.5 \times 10^{-19} n_N \frac{u^3}{\omega_c^2} \quad ,$$

where n_N is the total density of neutral atoms equivalent in cross-section to the oxygen atoms collided by 8keV electrons.

The beam radius expands following the relation

$$r = \{a_0^2 \xi_c^2 + 4D_\perp t\}^{1/2} \quad . \tag{7}$$

The diffusion process dominates after $\tau_3 = a_0^2 \xi_c^2 / 4D_\perp$. If we use the same parameters as before and assume $n_N = 10^{10} cm^{-3}$, we obtain

$$r = 1.6 \times 10^3 \; [\; 1 + 19t \;]^{1/2} \; cm \quad ,$$

and $\tau_3 \sim 50$ msec. Beacuse we have assumed that B and n_N are constant, the beam should be ejected at an altitude high enough for the expression (7) to apply in the scale length of $u\tau_3 \sim 3000$km. As far as the experiments are made within tens of kilometers of the shuttle, the beam radius can be approximated to $a_0 \xi_c$.

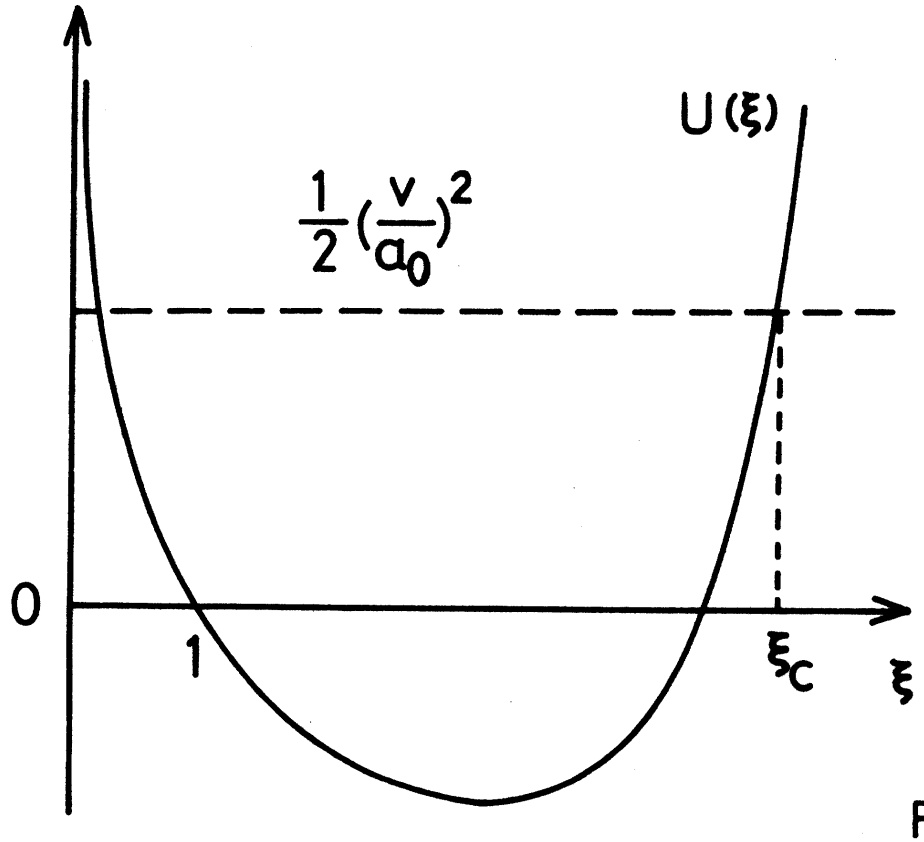
U(ξ)
$\frac{1}{2}(\frac{v}{a_0})^2$
0
1
ξ_c
ξ

FIG. 1

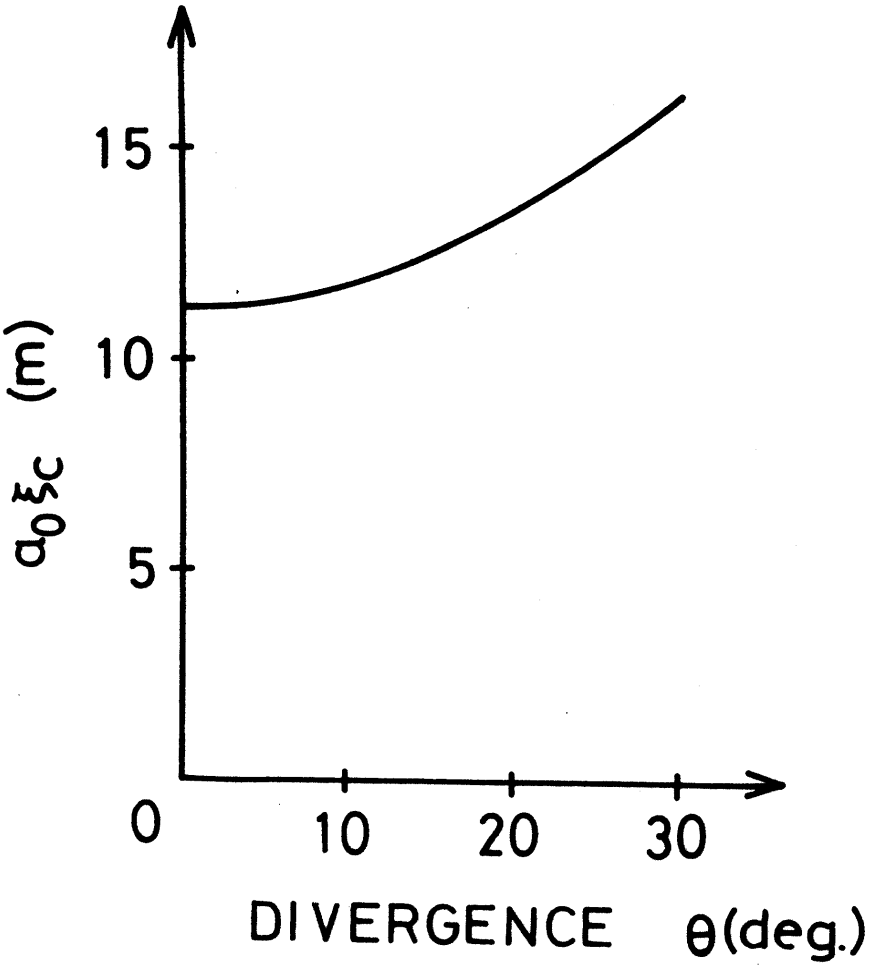
15
10
5
0
10
20
30
$a_0\xi_c$ (m)
DIVERGENCE θ(deg.)

FIG. 2

A Model of the Radio Emission Mechanism in Pulsars

KENJI KAWAMURA and IKURO SUZUKI
Department of Physics, Nagoya University

1. Introduction

Scargle and Pacini(1971) suggested that the crab pulsar contains a plasma or plasma clouds in the magnetosphere. Some aspects of the magnetosphere embedded in a plasma were investigated by Roberts and Sturrock (1972, 1973). On the other hand the possibility of outflows of high-energy electrons and positrons, which are created in pairs by energetic gamma rays, has also been pointed out by Sturrock(1970) and others.

Because of the strong magnetic field, particles lose their transverse energies rapidly, and consequently they can be regarded to form a non-gyrating beam.

In this report, we discuss that electromagnetic interactions between such a beam and the plasma provide a possible mechanism for pulsar radio emission. For simplicity we consider the simultaneous excitations of R and L waves by ultrarelativistic beams of electrons and positrons.

2. Beam Instability

Let us assume the distribution functions for the elctrons and positrons as

$$f_b(p_\perp, p_z) = \frac{\delta(p_\perp)}{\pi p_\perp} g(p_z) \quad . \tag{1}$$

Then, from the well-known dispersion relations, we obtain the growth rates for the R and L waves as

$$\delta^{\pm}_{\omega} = \frac{\pm\kappa\cdot\pi\cdot\tilde{\omega}_p^2\cdot\omega_H}{\frac{\partial}{\partial\omega}(\omega^2 n_\pm^2)} \frac{g(p_r)}{|p_r\omega-\gamma_r kc|} \quad . \tag{2}$$

Hereafter the momentums are scaled in units of m_0c, $\omega_H = |eB/m_0c|$, $\tilde{\omega}_p$ the plasma frequency of the beam, p_r is the root of $\gamma_r\omega - kcp_r \pm k\omega_H = 0$ with $\gamma_r = (1+p_r^2)^{1/2}$, κ denotes the sign of the beam charge, and $n_\pm$ the refractive indices of the plasma for the R and L waves. It is apparent from eq.(2) and the resonance condition that the L wave can be excited only by electron beam, and at the same time the velocities of the beam must be greater than the phase velocity (Zheleznyakov 1970). Similarly, the positron beam can couple with and excite only the R. Wave.

3. Model

We will assume that non-gyrating, high-energy beam of electrons and positrons flow outwards along open field lines. The beam will then interact with approximately stationary plasmas sorrounding and corotating with the central star.

For the present mechanism to give two orthogonally polarized subpulse such as suggested by Manchester et al.(1975), the emissions of radio pulses must occur in the region where both R and L waves become unstable. Namely the wave-frequencies must be smaller than the local ion gyrofrequency Ω_H. With a hydrogen plasma and from comparison with observed frequency range 10^2~10^3MH$_z$, it follows that the field strength B_s in the emitting region must satisfy the condition $B_s \gtrsim 10^6$G. Using the approximate resonant condition $\bar{\gamma}(n_\pm - 1) \sim \omega_H/\omega$, the above condition gives $N_s \gtrsim 2\ 10^{27} \times \omega^{-1} \bar{\gamma}^{-1}$. Here N_s is the particle density of the plasma, $\bar{\varepsilon} = \bar{\gamma} m_0 c^2$ the mean energy of the beam, and we used $(n_\pm - 1) \sim (c/v_A)^2/2$ which will be valid for the case $(c/v_A)^2 \ll 1$ and $\omega < \Omega_H$. With $\omega/2\pi \sim 500$MH$_z$ and $\bar{\gamma}_{max} \sim 10^7$, we have the restriction $N_s \gtrsim 5 \times 10^{10}$cm^{-3} for our mechanism to work.

For our estimates, we will assume $B_s \sim 10^6$G, which corresponds to the distance $r_s \sim 10^8$cm as a dipole field, and $\bar{\gamma} \sim 10^5$, hence $N_s \sim 5 \times 10^{12}$cm^{-3}. Then the growth rates become $\delta_\omega^\pm \sim 2\ 10^{-5} (N_b/\eta)$, where N_b is the particle density of the beam. We here also use the approximation $g(p_z) \sim 1/\eta \cdot \bar{\gamma}$, where $\eta = \Delta\gamma / \bar{\gamma}$. With $N_b \sim 10^{10}$cm^{-3} and $\eta \sim 1$, $\delta_\omega^\pm \sim 2\ 10^5$s^{-1}, and in the linear approximation the waves will be amplified by a factor exp(100) after the passage of the distance 10^7cm.

The particle density of the beam assumed here is high but compatible with the analysis by Hankins and others (Hankins 1971, 1972; Rickett et al. 1975). According to them, it is suggested that typical pulse results from a group of small emitting regions corresponding to observed micropulses. Considering an oblique rotation with an angle χ and using energetic consideration, the particle dinsity is then estimated as

$$N_b \leq \frac{32}{5}\pi \frac{MR^2}{N(v_s \Delta t)^2 \bar{\varepsilon} \cdot c} \frac{|\dot{p}|}{p^3} \quad . \tag{3}$$

Here N is the number of small emitting regions, $v_s \sim r_s \sin\chi \cdot (2\pi/p)$, p the pulse period, and Δt the duration of a micropulse. For $\bar{\varepsilon} = \bar{\gamma} m_0 c^2 \sim 10^5 m_0 c^2$, $M \sim 1 M_\odot$, $R \sim 10^6$, $\chi \sim \pi/4$, $r_s \sim 10^8$cm, $p \sim 0.5$s, $\dot{p} \sim -6 \times 10^{15}$ and $\Delta t \sim 200\mu$s for pulsar

PSR 0950, we obtain $N_b \lesssim (3/N)\times 10^{13}\,cm^{-3}$. If we assume that a few percent of the rotational energy-loss can be converted into the beams and $N \sim 10^2$, we will obtain $N_b \sim 10^{10}\,cm^{-3}$ assumed here.

4. Brightness Temperature and Spectrum from the Model Pulsar

If the plasma layer sufficiently extends, say $\gtrsim 10^7$ cm, the final state of the excited waves, which will be determined by nonlinear effects, should be compared with observations. To estimate this, we use the quasilinear approximation for the cyclotron instability (Rowlands et al. 1966). In the present case, we must include relativistic effects, however the refractive index will be assumed to be constant for $\omega < \Omega_H$. Then an asymptotic solution of the quasilinear system is found out analytically (Kawamura and Suzuki 1976). The results for a stationary state are

$$\varepsilon_\omega(z=\infty) = \frac{m_0^2 c^2 \omega_H^2 \tilde{\omega}_p^2}{4e^2 (n^2-1)^2 \omega^2} \int_{\psi_1(\omega)}^{\infty} d\psi \int_{\omega}^{\omega_{max}} d\phi \; \frac{p_z(\phi,\psi)}{\phi^2} \left[f_b(z=\infty) - f_b(z=0) \right] \tag{4}$$

and

$$f_b(z=\infty) = \int_{\phi_{min}(\psi)}^{\omega_{max}} d\phi \; \frac{p_z(\phi,\psi)}{\phi^2} \, f_b(z=0) \Big/ \int_{\phi_{min}(\psi)}^{\omega_{max}} d\phi \; \frac{p_z(\phi,\psi)}{\phi^2} \,. \tag{5}$$

Here $\phi_{min}(\psi) = \omega_H / [n^2\psi^2 - (n^2-1)]^{1/2}$, $\psi_1(\omega) = [(\omega_H/\omega)^2 + n^2 - 1]^{1/2}/n$, and ϕ and ψ are independent variables defined by the following relations,

$$\phi = \frac{\omega_H}{n \cdot p_z - (1+p_\perp^2+p_z^2)^{1/2}}, \qquad \psi = (1+p_\perp^2+p_z^2)^{1/2} - \frac{p_z}{n} \,. \tag{6}$$

To estimate the brightness temperature, we, for simplicity, use mono-energetic beam, i.e., $f_b(z=0) = \delta(p_\perp)/\pi p_\perp \cdot \delta(p_z - p_z^*)$. Then we can easily obtain the final spectrum. The corresponding brighteness temperature T_b can be approximately expressed as

$$T_b \sim \frac{4}{3}\pi^2 \frac{m_0^2 c^5 \tilde{\omega}_p^2 \cdot \omega_H^2 \, (1+\omega_H/(n^2-1)\omega p_z^*)}{k e^2 (n^2-1)^2 \omega^5 p_z^*} \,, \tag{7}$$

where k the Boltzmann constant. For $n^2 - 1 \sim 10^{-1}$, $N_b \sim 10^{10}\,cm^{-3}$, $p_z^* \sim 10^5$, $B \sim 10^6$ G and $\omega/2\pi \sim 600\,MH_z$, we obtain the maximum temperature of the order $T_b \sim 4\times 10^{290}$ k. This value is compared with the value of the order 10^{30} k suggested by Hankins (1971, 1972).

To compare the spectrum obtained with observations, we assume the distribution function in the form $f_b(z=0) = \delta(p_\perp)/\pi p_\perp \cdot g(p_z)$. We here

cosider the two different cases for $g(p_z)$, i.e.,

$g(p_z) = (1/\sqrt{\pi}\Delta_z)\exp[-\frac{(p_z-p_z^*)^2}{\Delta_z}]$ and $g(p_z) = \text{const}\cdot[p_z^{-\alpha} - p_2^{-\alpha}]$ for $p_1 \leq p_z \leq p_2$ and $\alpha > 0$. By using the same procedure as before, it follows that the spectra display low-frequency turnover and approximatly decrease with ω^{-3} in the high-frequency range. Such a stectral behavior appears to give a good fit to some pulsar spectra. In fig.(1), the spectrum for the Gaussian distribution is shown together with the spectrum of PSR 0833 for $\Delta_z/p_z^* \sim 0.5$ and other parameters as before. In fig(2), the spectrum for the power-law case is displayed together with the spectrum of PSR 2016 for $\alpha = 1.3$, $p_1 \sim 1\times10^4$, and $p_2 \sim 1\times10^6$.

5. Discussion

In the present model parameters, an electrostatic instability need not be taken into account. With a cold beam, the ratio δ^e/δ^t is of the order $(N_s/N_b)^{1/6}(\omega/\omega_H)^{1/2}$. For $\omega \sim 10^9 H_z$, $B_s \sim 10^6 G$ and $N_b/N_s \sim 2\ 10^{-3}$, $\delta^e/\delta^t \sim 4\times10^{-2}$. Also, the cyclotron absorption, which occurs in escaping from the magnetosphere, may be determined by the nonlinear effects (Palmadesso and Schmidt 1971).

Refferences

Hankins,T.H., 1971, Ap.J, 169 487.

Hankins,T.H., 1972, Ap.J, (Letters), 177, L11.

Kawamura.K and Suzuki.I., 1976, submitted to Ap.J.

Manchester,R.N., Taylor,J.H. and Huguein,G.R., 1975, Ap.J., 196, 83.

Palmadesso,P. and Schmidt,G., 1971, Phys. Fluids 14, 1411.

Rickett,B.J., Hankins,T.H. and Cordes,J.M., 1975, Ap.J.

Roberts,D.H. and Sturrock,P.A., 1972, Ap.J.,(Letters), 173, L33.

1973, Ap.J., 181, 161.

Rowlands,J., Shapiro,V.D. and Shevchenko,V.I., 1966, J.E.T.P., 23, 651.

Scargle,J.D. and Pacini,P., 1971, Nature, 232, 144.

Sturrock,P.A., 1970, Ap.J., 164, 529.

Zheleznyakov,V.V., 1970, Radio Emission of the Sun and Planets (Oxford; Pergamon Press).

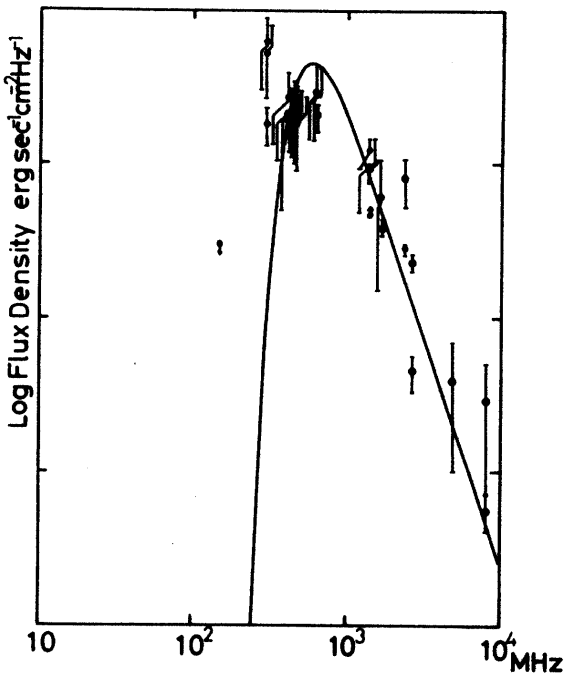
Log Flux Density ergsec⁻¹cm⁻²Hz⁻¹
10
10²
10³
10⁴MHz

Fig. 1

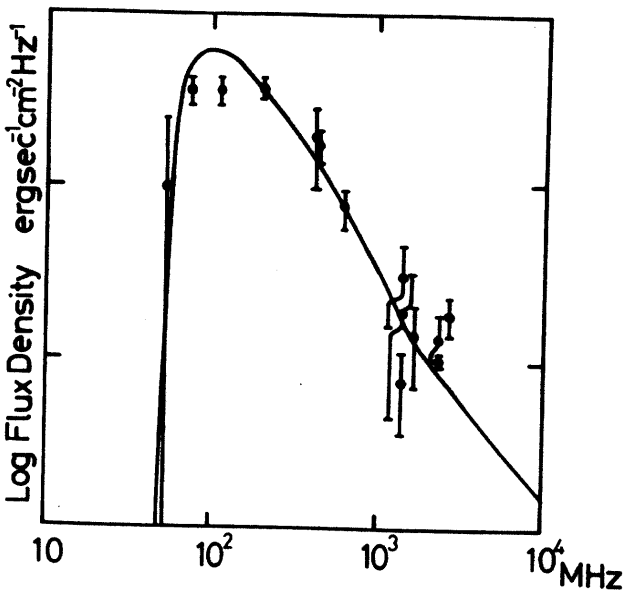
Log Flux Density ergsec⁻¹cm⁻²Hz⁻¹
10
10²
10³
10⁴MHz

Fig. 2

A MODEL OF JOVIAN SHORT-DURATION BURSTS

KENJI KAWAMURA and IKURO SUZUKI

Departmnet of Physics, Nagoya University

1. Introduction

Jovian short-duration bursts are roughly characterized by fast frequency drifts, narrow bandwidth, high brightness temperatures, and polarization properties with strong circular components whose sense is right-handed above 20 MH_z (Ellis, 1965; Warwick, 1967; Zheleznyakov, 1970; Ellis, 1974). As a candidate for the emission mechanism of the bursts, Ellis (1965) has suggested an electromagnetic cyclotron instability due to mono-energetic gyrating beams trapped in the magnetosphere.

The purpose of this report is to show that the mechanism actually explains some aspects of S bursts quantitatively. For this, a wave propagation is assumed to be longitudinal, and the gyrating beam is assumed to be almost mono-energetic initially. These are likely to be acceptable in the present case.

2. Electromagnetic Instability

In the present model, we consider the case of $\tilde{\omega}_p^2 \ll \omega_p^2$, and hence the real part of the wave-frequency will be completely determined by the ambient plasma. Here $\tilde{\omega}_p$ and ω_p denote the plasme frequency of the beam and the plasma, respectively. With a mono-energetic gyrating beam, the growth rate is then given by

$$I_m\delta = \frac{\sqrt{3}}{2}\left[\frac{\beta_\perp^2\tilde{\omega}_p^2\Omega^2|n^2-1|}{2\gamma\frac{\partial}{\partial\omega}(\omega^2n^2)\Big|_{\omega=\Omega}}\right]^{1/3}, \qquad (1)$$

where $\beta_\perp = v_\perp/C$, n the refractive index of the plasma for the R wave, γ the Lorentz factor, and Ω the real frequency. In deriving eq.(1), we assumed the following conditions:

$$\Omega^2 \cdot n^2 >> |\delta| \cdot \frac{\partial}{\partial\omega}(\omega^2 n^2)\Big|_{\omega=\Omega} , \tag{2}$$

$$\Omega^2 |n^2 - 1| >> 2\Omega|\delta| , \tag{3}$$

and

$$\frac{1}{2}\beta_\perp^2 \Omega^2 |n^2 - 1| >> \omega_H |\delta| . \tag{4}$$

The instability can take place for both fast and slow waves corresponding to $n < 1$ and $n > 1$, respectively. From the viewpoint of escaping from the magnetosphere, we here consider only the fast waves with $\omega > \omega_H$, and then, as easily seen from the resonance condition, the beam must stream in the same direction as the waves propagate.

The above results were derived for the entirely cold beam. However they may be also applicable for the actual beam with velocity spreads $\Delta\beta_\perp$, $\Delta\beta_z$, when the autocorrelation time is small compared with the characteristic time of the wave-growth (Tsytovich, 1970). For the nonrelativistic case, the condition may be written down as

$$\Delta\omega \left|1 - \bar{\beta}_z \cdot C/v_{gr}\right| \sim \left|\omega[\bar{\beta}_\perp \cdot \Delta\beta_\perp + \bar{\beta}_z \cdot \Delta\beta_z] - k_c \Delta\beta_z\right| << I_m \delta . \tag{5}$$

3. Numerical Examination

We here seek the plasma parameters required from the conditions (2)-(4) and observational data. For this purpose, we assume the ambient plasma as cold and set $\Omega - \omega_H = \eta \cdot \omega_p$. For the case of $\omega_p/\omega_H \lesssim 0.1$ and $\eta \lesssim 1$ that is likely to hold in Jovian magnetosphere, Ω will be well approximated by ω_H except for $\Omega - \omega_H$. Using the resonance condition, we have the following, approximate equation for η;

$$\eta^3 - \beta_z^2(\omega_H/\omega_p)^2\eta + \beta_z^2(\omega_H/\omega_p) = 0 \qquad (6)$$

On the other hand, β_z is related with frequency-drift observation, nemely,

$$\beta_z \sim \frac{1}{3}\frac{R_j}{\omega_H \cdot C}(-d\omega/dt) \qquad (7)$$

where R_j the radius of Jupiter. Thus, if the $(d\omega/dt)$ and the plasma parameters are given, the acceptable beam parameters, and hence the growth rate, will be determined by the conditions (2) - (4)

For our estimates, we assumed $\Omega \sim \omega_H = 56\pi MH_z$ and $\omega_p/\omega_H \sim 7.1\times10^{-2}$, i.e., the field strength $B_0 \sim 10G$ and the particle density $N_0 \sim 5 \times 10^4 cm^{-3}$. We also use $(-d\omega/dt) \sim 10MH_z/s$ (Ellis, 1974). From eqs.(6) and (7), we then obtain $\beta_z \sim 3 \times 10^{-2}$ and two acceptable values for η , i.e., $\eta_1 = 8 \times 10^{-1}$ and $\eta_2 = 3.3 \times 10^{-1}$. We furthermore substitute the above values into the conditions (2) - (4), and then it follows that, as an example, the values of $\beta_i \sim 0.5$ and $N_b \sim 10^{-2}\ cm^{-3}$ satisfy the conditions. The growth rates corresponding to η_1 and η_2 are of the order of $\delta_1 \sim 1.3 \times 10^4$ and $\delta_2 \sim 2.1 \times 10^4$, respectively. Since a single-frequency duration Δt of S bursts is of the order $1 \sim 10ms$(Ellis, 1974), Wave energies may be enormously amplified in a linearized regime.

However, as we shall see below, the velocity spreads of the beam will rapidly increase because of the reaction due to the excited waves, and consequently the hydrodynamic approximation used here will break down to go over to the kinetic stage. It seems that the instability for the fast waves scarcely occurs in that stage (Chang 1964). Therefore it is expected that the energy transfer from the beam to the waves will mainly take place in the hydrodynamic stage. The narrow-band character of S bursts appears to support this expectation.

4. Evolution of The Beam

The equation describing the slowly varying part of the beam distribution function can be derived in the standard manner (See, for example, Davidson, 1972). By taking the moments of the equation, we see that, the slow variation of the mean value of $Q(P_\perp, P_z)$ can be descirbed by

$$\frac{\partial}{\partial t} N_b \langle Q \rangle = \left(\frac{2\pi e}{m_0 c}\right)^2 R_e \; i \sum_k \varepsilon_k \int_0^\infty dp_\perp \int_{-\infty}^\infty dp_z \Big[\frac{1}{(\omega_k - kc\frac{p_z}{\gamma} - \frac{\omega_H}{\gamma})} \Big\{ \frac{kc}{\omega_k} \frac{p_\perp}{\gamma} \frac{\partial S}{\partial p_z} + (1 - \frac{kc}{\omega_k} \frac{p_z}{\gamma}) \frac{\partial S}{\partial p_\perp} + \frac{p_\perp}{\gamma^2} S \Big\} + \frac{1}{(\omega_k - k_c \frac{p_z}{\gamma} - \frac{\omega_H}{\gamma})^2} \times \frac{(kc)^2 - \omega_k^2}{\omega_k} \cdot \frac{p_\perp}{\gamma^2} \cdot S \Big] F(p_\perp, p_z), \tag{8}$$

where $S = \frac{\partial}{\partial p_z}\left(\frac{kc}{\omega_k} \cdot \frac{p_\perp^2}{\gamma} \cdot Q\right) + p_\perp \frac{\partial}{\partial p_\perp}\left(1 - \frac{kc}{\omega_k} \frac{p_z}{\gamma}\right) Q$.

For order of magnitude-estimate, we approximate the distribution function F in the right-hand side by cold one. Using eq.(8) and taking $v_\perp = \frac{p_\perp c}{\gamma}$, and $v_\perp^2$ as Q, we have the following equation for the transverse spread;

$$\frac{\partial}{\partial t} N_b \langle \Delta v_\perp^2 \rangle = \frac{\tilde{\omega}_p^2}{2m_0} \sum_k \frac{(1 - \frac{kc}{\Omega} \beta_z - \beta_\perp^2)^2 \cdot \frac{\partial \varepsilon_k}{\partial t}}{\gamma^2 \{ (\Omega - kc\beta_z - \frac{\omega_H}{\gamma})^2 + \delta_k^2 \}} . \tag{9}$$

Similarly, we can easily obtain the equation for the longitudinal spread. Since

$$\frac{\partial}{\partial t} N_b \langle \Delta v_z^2 \rangle / \frac{\partial}{\partial t} N_b \langle \Delta v_\perp^2 \rangle \sim \beta_\perp^2 (kc/\Omega - \beta_z)^2 / (1 - \beta_z kc/\Omega - \beta_\perp^2)^2 ,$$

the ratio is very small for the present case $\beta_z \ll 1$, $\beta_\perp \ll 1$, and $kc/\Omega < 1$, and hence we conclude that the variation of the transverse spread plays a major role in the development of the beam.

Now we assume that both spreads of the beam satisfy the condition

(5) initially, and afterward the beam will mainly evolve according to eq.(8). As estimated form eq.(5), when the transverse spread is extended to the order $\Delta\beta_\perp \sim \delta_k/\beta_\perp \cdot \Omega$, the hydrodynamic stage will break down as pointed out by Toytonick in an electrostatic case. To estimate the maximum wave-energy acquired, we integrate eq.(8) with respect to t and substitute $\Delta\beta_\perp \sim \delta_k/\beta_\perp \cdot \omega$ into the resultant. Expressing it in terms of the brightness temperature T_b, we finally obtain the following, approximate expression;

$$K \cdot T_b \sim 3\sqrt{3} \cdot \pi^3 \cdot \frac{1}{\Omega}\left(\frac{c}{\Omega n}\right)^2 \left|n^2-1\right| \cdot \left|v_{gr} - \beta_z c\right| m_0 N_b c^2 \ . \qquad (10)$$

For the same parameters as before, the brightness temperatures are of the order of 8×10^{16}K for η_1 and 5×10^{15} K for η_2. Since the present estimate gives the upper limit of the temperature, our estimate well agrees with Warwick's (1967) one $10^{14} \sim 10^{15}$K.

5. Discussion

In the present case, the growth rate for longitudinal waves considerably exceeds that for the transverse waves. However to compare efficiencies of the wave-excitation in two cases, the effects of phase mixing must be taken into account as pointed out by Bell and Buneman (1964). According to them, we may take $R=\delta/k \cdot \Delta v_z$ as a rough measure of the efficiency. Then $R_t/R_\ell \sim (\beta_\perp/\eta)^{2/3}$, and when $\beta_\perp > \eta$, the electrostatic instability will not play a major role. For the above parameters, this requirement is satisfied.

References

Bell, T.F., and Buneman, O., 1964, Phys. Rev., 133, A1300.
Chang, D.B., 1963, Ap. J., 138, 1231.
Davidson, R.C., 1972, Methods in Nonlinear Plasma Theory, Academic Press.
Ellis, G.R., 1965, Radio Science, 69D, 1513.
Ellis, G.R., 1974 Astronomical Society of Australia, 2, 236.
Kawamura, K., and Suzuki, I., 1976, Astrophys. Letters. 18, 19.
Tsytovich, V.N., 1970, Nonlinear Effects in Plasma, Plenum Press.
Warwick, J.W., 1967, Space Sci. Rev., 6, 841.
Zheleznyakov, V.V., 1970, Radio Emission of The Sun and Planets, Pergamon Press.

REB Interaction Experiments with Plasmas

S. Nakai, K. Imasaki, S. Miyamoto and
C. Yamanaka
Institute of Laser Engineering,
Osaka University
Osaka, Japan

1. Introduction

The spherical ablation to compress and to ignite thermonuclear burn of a fuel pellet depends upon an efficient dissipation mechanism to deposit most of the electron beam energy symmetrically in the outer thin portion of a target.
We have investigated the energy deposition mechanisms when a tightly focused beam has been irradiated onto a plane solid low Z target.[1][2][3] The results shows the existence of an anomalously stronger interaction than classical one.

2. Experimental Apparatus

We have constructed REB generators REIDEN-I, II,and III. They are consisted of a Marx-generator, a Blumlein type pulse forming line and a diode. In REIDEN-I, a paralell plate Blumlein with mylar insulator are used. Coaxial Blumlein of water insulator are used in REIDEN-II and III. Most experiments on REB-plasma interaction have been done by using REIDEN-II and III. The characteristics of them are shown in Table 1.

The diagnostic methods for beam and plasma are as follows. The voltage wave form across the diode and the beam current are monitored by a resistive divider and a current shunt of toroidal resistor on the return path from the target respectively. The response times of them has been checked to be less than 10 nsec. The focal spot size of the beam on the target is estimated from the X-ray image of 3 channel pinhole camera with Be-foil of different thickness as an X-ray absorber, with the assistance of the observation of the plasma by a high speed streak camera. An electric image converter framing camera (5 nsec exposure time) is also used

to observe the dynamical behavior of plasmas. The electron temperature of plasmas is estimated by 2 channel X-ray absorbing foil detectors of 200 μm and 400 μm Be-foils. The ion velocity is measured by the time of flight method. Two charge collectors are set at the position of 68 cm and 33 cm distant from the focal spot of the beam on the target. The total neutron yield is counted by paraffin moderated activation of Dysprosium which has been calibrated by AmBe neutron source. Neutron energy is measured by time of flight method using two plastic scintillation neutron counter located at the position of 4 m and 9 m distant from focal point of the beam.

3. Experimental results

3.1 Plasma production and heating

When focused beam bomobards the target, plasma is produced at focal point. The size of bright spot corresponds to that of image of hard X-ray which is identified as the size of beam focusing. Then the plasma expands along the target surface and does not expand toward cathode.[1] This behavior is due to the magnetic pressure of the beam current.

Fig. 1 shows the time variation of measured electron temperature of the polyethylene target plasma assuming Maxwellian velocity distribution of electrons for 200 KeV, 40 KA beam bombardment. The electron temperature at 50 nsec from pulse rise is about 8 KeV. At the later time than 150 nsec it decays exponentially. The voltage pulse ended at about 80 nsec but the current continued to flow for about 150 nsec. During the current flowing, the X-ray due to the beam current overlaps to the X-ray from the plasma, so the electron temperature is overestimated. The real electron temperature of plasma just after the pulse is estimated as 1~2 KeV by extrapolation of decay curve in Fig. 1

The ion velocity is measured by the time of flight method. Using a polyethylene tharget the ion kinetic energy of the carbon is about 1~2 KeV for the case of Fig. 1 For Al and Pb targets, the dependence of the expanding velocity of the ions on the diode voltage is shown in Fig. 2 where the solid line is the calculated value assuming the beam plasma interaction to be classical one.

3.2 Neutron generation

When the plasma temperature is so high as a few KeV with the density comparable to solid, we can expect neutron generation by thermonuclear reaction. Only in that case when CD_2 target is used, neutron generation is observed. The neutron signals on the scintillation detectors at the location of 4 m and 9 m distant from the focus point are shown in Fig. 3 The energy of neutron are identified to be 2.45 MeV, which is consistent with that of D-D reaction. The dependense of neutron yield on the electron beam power are plotted in Fig. 4 with CD_2 thin film target of the thickness of 100, 160, 200 and 300 μm. It should be noticed that there are no difference in neutron yield depending on the different thickness of target.

4. Discussion

When an electron beam impinges on solid target, it heats, evaporates and ionizes the target material. The main deposition mechanism of beam energy is via beam-plasma interaction. Assuming that the electron beam of radius r is stopped in range λ over which the electrons lose their energy, the plasma temperature T may be given approximatly by the energy balance equation

$$\pi r^2 \lambda n_1 kT \simeq IV\tau \qquad (1)$$

where n_1 is the plasma density which interacts with the beam, k is the Boltzmann constanat, I is the beam current, V is the beam accerelation voltage and τ is the pulse length of the beam when it is short enough to neglect the plasma motion or the expansion time of plasma from the electron beam radius. Here the energy loss by radiation and thermal conduction is neglected.

There are several possible mechanisms for the energy deposition of the beam tc the plasma to estimate the range λ. They are the classical process of binally collision and Čerenkov radiation, two stream instabilities in hydrodynamic and kinetic instability depending on the beam properties, and the return current instability.

The energy loss of the beam by Coulomb scattering gives the range of about 1.5 mm for 200 KeV electron in polyethylene target. With this value of range eq. (1) gives about 20 eV as the plasma temperature for the same condition of Fig. 3, which is two order

of magnitude lower than the measured value. Such a long range can not explain the observed neutron production with thin CD_2 target of 100 to 300 μm.

In the high density plasma of $10^{19} \sim 10^{22}$ cm^{-3}, the electron drift velocity due to return current hardly exceeds the ion acoustic velocity. Therefore this mechanism can not contribute to the energy deposition of the beam electrons in solid target experiments.

As for the two stream instability in cold beam-cold plasma, the maximum growth rate is given by[4]

$$\sigma = 0.7\left(\frac{n_2}{n_1}\right)^{1/3} \omega_{pl} \qquad (2)$$

where ω_{pl} is the electron plasma frequency corresponding to the plasma density n_1 and n_2 is the beam electron density. Assuming that the stopping length of the beam electron is given by

$$\lambda = \frac{v_e}{\sigma} \qquad (3)$$

where v_e is the beam electron velocity, eq. (1) predicts quite reasonable value of plasma temperature comparing to the experimental results. In this calculation, the plasma density n, is taken to be solid density $\sim 10^{22}$ cm^{-3}. In the solid density plasma the damping rate of beam driven plasma instability is marginal comparing to the growth rate even with the low Z hydrogen plasma at temperature of 1~2 KeV. In general the thermal expansion of plasma can not be neglected when longer pulses than 10 nsec are used. Therefore interaction in the expanding corona region must be considered. If we apply the hydrodynamic instability to the corana region, the plasma temperature becomes much higher than the observed value.

In the strongly focused beam the hot beam condition will be fulfilled for the applicability of the kinetic instability,[5] that is

$$\Delta\theta \gtrsim \max\left\{\left(\frac{n_2}{n_1\gamma}\right)^{1/4}; \left(\frac{n_2}{n_1\gamma^3}\right)^{1/6}\right\} \qquad (4)$$

The growth rate of instability with the beam of the velocity spread $\Delta\theta$ is given by

$$\sigma = \omega_{pl} \frac{n_2}{n_1 \gamma} \frac{1}{\Delta\theta^2} \frac{\omega_{pl}^2}{\omega_{pl}^2 + k_\perp^2 c^2} \qquad (5)$$

Using equation (1) (3) and (5), we can estimate the plasma temperature, which agrees quite well with the observed value when the plasma density n_1 is taken to be 5×10^{19} cm^{-3} where the electron beam mainly interacts. The neutron yield can be estimated by

$$N = \frac{1}{2} n_D^2 \langle \sigma v \rangle \pi r^2 \lambda \tau_r \qquad (6)$$

Putting the parameters in experiments for r = 1.5 mm, τ_r = 180 nsec, the yield of neutron is calculated as shown in Fig. 4 using the integrated fusion cross section $\langle \sigma v \rangle$ over Maxwell distribution corresponding to the derived temperature by eq. (1). It is obviously noticed that the neutron yield and the dependence on input beam power are consistent with the experimental results

In the REB-target interaction, the boundary and interaction region may be very complicated. The self magnetic field of REB may be shielded by the magnetic skin depth $\delta = c\tau^{1/2}(4\pi\sigma)^{-1/2}$ which is 3×10^{-3} cm for the plasma of 1 KeV temperature and the injection time of τ = 10 nsec. The density gradient of the plasma in corona region must be estimated including the kinetic and magnetic pressures of the beam, and its balance with the pressure of expanding plasma.

5. Conclusion

The experimental results presented here, such as neutron yield, plasma temperature and kinetic energy, show the existence of anomalously strong interaction of REB with low Z dense target plasma. The REB dissipates most of it energy in the thin layer or in corona region and does not penetrate deeply into the target material. This fact is favorable for the pellet fusion by the implosion using the intense focused REB.

REFERENCES

(1) K. Imasaki, S. Nakai and C. Yamanaka: Jour. Phys. Soc. Japan 37, 881 (1974)

(2) K. Imasaki, S. Nakai and C. Yamanaka: ibid 38, 1554 (1975)

(3) K. Imasaki, S. Miyamoto, S. Nakai and C. Yamanaka: ibid 40, 531 (1976)

(4) O. Buneman: Phys. Rev. 115, 503 (1959)

(5) B. N. Brejzman and D. D. Ryutov: Nuclear Fusion 14, 873, (1974)

Table 1

	Type	Pulse length	Impedance	Marx bank	Typical performance	Focus spot	Power density
REIDEN II	Water coax. blumlein	100nsec	13Ω	400kV 10kJ	300kV 20kA	1mm	6×10^{11} W/cm^2
REIDEN III	Water coax. blumlein	80nsec	2Ω	900kV 27kJ	500kV 80kA	1.5mm	2×10^{12} W/cm^2

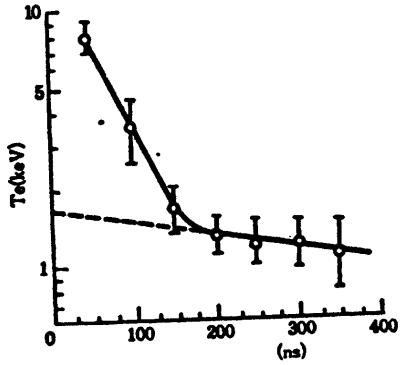

Fig. 1 Electron temperature of plasma as a function of time

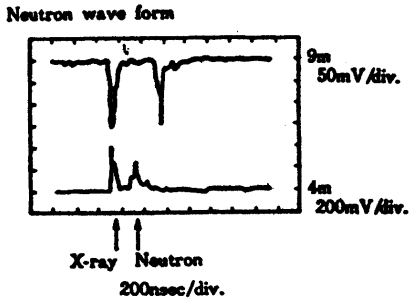

Fig. 3 Neutron signal on plastic scintillation counter

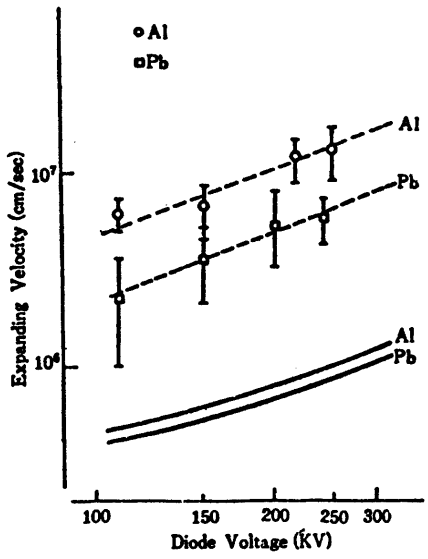

Fig. 2 Ion velocity measured by time of flight method

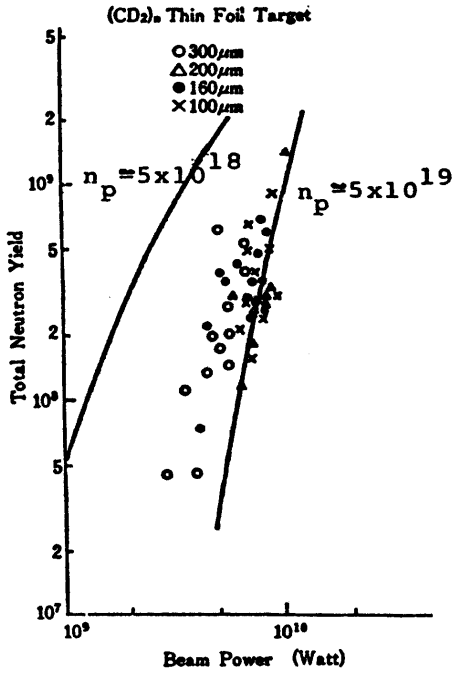

Fig. 4 Dependence of neutron yield on beam power for the CD_2 target of various thickness and estimated value (solid line).

Experiments on Relativistic Electron Beam at the Institute of Plasma Physics, Nagoya University

A. Mohri

There has been an increased interest in the application of intense relativistic electron beams and energetic ion beams to controlled nuclear fusion and plasma physics. The research of these objectives at the institute first began in 1970, and since then efforts have been devoted to the study of REB generation and the injection of REB into toroidal and mirror devices. An ERA device, toroidal devices (SPAC-2, 3 and 4) and several REB sources (coaxial Marx generators, Phoebus-1) were constructed. A REB source of medium size named Phoebus 2 was designed and its construction is now nearing completion. After comissioning the source will be used for further experiments on the formation of REB rings for plasma confinement and also for the generation of ion beam generation. Parameters of these devices are listed in Table 1.

Table 1. Experimental devices for researches of REB at IPP-Japan

I. REB sources

	output voltage	energy of capacity bank
coaxial Marx generator	2 MV	1 kJ
	750 kV	560 J
	600 kV	150 J

	beam energy	total energy	current	pulse width
Phoebus-1	400 keV	1 kJ	80 kA	25 ns
Phoebus-2	800 keV	7 kJ	260 kA	60 ns

II. Toroidal devices

	major radius	minor radius	shape of shell	B_t	B_r
SPAC-2	28 cm	5.5 cm	circular	20 kG	0.2 kG
3	12 cm	6 cm	rectangular	2 kG	0.5 kG
4	5 cm	5 cm	spherical	1 kG	2.0 kG

Formation of toroidal high currents of relativistic electron beam (REB ring) will offer new potential for plasma confinement. The diffusion of magnetic field in high magnetic shear systems like the reversed field pinch is much suppressed if the usual plasma current is replaced with the REB ring. Toroidal devices of very small aspect ratio are realizable and the plasma heating by three-dimensional adiabatic compression can be applied effectively. Experiments in SPAC-2, 3 and 4 have proved that the state of the safety factor $q < 1$ can be realized by the injection of REB and the system is stabilized by keeping the magnetic shear. New device SPAC-5 is now under construction for further study of the adiabatic compression.

The institute has a programme to produce an ambi-plasma which is composed of positrons and electrons. The density of the ambi-plasma up to $10^{11\sim12}$ cm^{-3} will be attained by irradiating intense X-rays on a lead target. To produce the X-rays, a large REB source is to be used which will be comissioned within the next year. Experiments on behaviours of ambi-plasma on the earth will offer a new means to understand astronomical phenomena such as the origin of pulser.

Dynamics of a Cloud of Fast Electrons Travelling Through the Plasma

T. TAKAKURA, Department of Astronomy, University of Tokyo

The aim of this study is to investigate the dynamics of solar electrons under the interaction with the plasma waves. Since the straightforward computer analysis of such a problem in a wide range of interplanetary space is not practical, two steps have been taken.

The first step is the computer analysis in a limited distance ($x \lesssim 10d$) from the electron source (radius d) setting rather low number density for the beam electrons in order to avoid too long computer time. It is shown that the electron velocity distribution $f(v,x,t)$ becomes quasi plateau during the time for which the plasma waves are strongly excited (Takakura and Shibahashi, 1976). The plasma waves are re-absorbed later by the following beam electrons with a negative $\partial f/\partial v$. On the other hand, the asymptotic plateau solution given by Ryutov and Sagdeev (1970) for $f(v,x,t)$ is modified taking into account both the collisional loss of beam electrons and the collisional decay of the plasma waves. Then the analytical and numerical results are compared at $x \simeq 10d$, showing rather good fitting (Takakura, 1976). Thus an approximate formula for the electron distribution function $f(v,x,t)$ can be given analytically.

The 2nd step is to compute the plasma waves $w(v,x,t)$ by

the use of the analytically given f(v,x,t). This computation can be easily made at any given x for the parameters which are directly applicable to the solar electrons. The effect of the scatterings of plasma waves into other plasma waves can be taken into account in this stage under the condition that the reaction of this effect on the electorn distribution is small.

One-dimensional equations for the quasi-linear diffusion of beam electrons in velocity space are given by

$$\frac{\partial f_s}{\partial t} + v\frac{\partial f_s}{\partial x} = \frac{\partial}{\partial v}\left[\left(\frac{2\pi e}{m}\right)^2 \frac{w}{v}\frac{\partial f}{\partial v} + \frac{(2\pi e\nu_p)^2}{mv^2}\ln\left(\frac{v}{v_0}\right) f_s + \nu_s v f_s\right], \qquad (1)$$

$$\frac{\partial w}{\partial t} = \frac{2\pi e^2}{m\nu_p} v^2 w\frac{\partial f}{\partial v} + 2\pi e^2 \nu_p v \ln\left(\frac{v}{v_0}\right) f_s - \nu_c w + Sc\cdot, \qquad (2)$$

where

f_s is velocity distribution of beam electron,
thermal electrons f_T are included in $f(=f_s+f_T)$,
w is spectral energy density of plasma waves,
ν_p is plasma frequency,
ν_s is collision frequency for beam electrons due to collisions with thermal electrons,
ν_c is collision frequency for thermal electrons and
Sc is scattering term for the plasma waves.
The terms including $\ln(v/v_0)$ in equations 1 and 2 are attributed to the Čerenkov emission (spontaneous emission) of plasma waves, where v_0 is the phase velocity below which

Landau damping becomes serious ($v_0 \simeq 4\ v_{Te}$). Note that a little modification of equation 1 is required if we take into account an increase with x of a cross-section of electron beam.

Substituting equation 2 into 1, we have

$$\frac{\partial f_s}{\partial t} + v\frac{\partial f_s}{\partial x} = \frac{\partial}{\partial v}\left[\frac{2\pi\nu_p}{mv^3}\left\{\frac{\partial w}{\partial t} + \nu_c w - Sc\right\} + \nu_s v f_s\right] \quad . \tag{3}$$

Equations 3 and 2 are solved numerically setting Sc=0 and assuming an initial distribution

$$f_s(0) \sim v^{-6} \exp\{-(x/d)^2\} \ , \qquad v>v_0 \qquad , \tag{4}$$

with an initial column density

$$N_0 = \int_{v_0}^{\infty}\int_{-\infty}^{\infty} f_s(0)\ dx\ dv \quad .$$

Two examples are shown in Figures 1 and 2 in which all quantities are dimensionless. Figure 1 shows a simplest case in which collisional terms are neglected and the beam density is low ($N_0=4\cdot10^9$ cm^{-2}). We can see the quasi-plateau appearing in a limited velocity and time ranges, and that the plasma waves are reabsorbed by the beam electrons due to a later appearance of negative ($\partial F/\partial V$) at any given V. Figure 2 shows the results for a final model in which ν_p decreases with x and a cross-section of electron beam increases with x; ν_s, $\nu_c \neq 0$. Solid curves and dotted curves are derived numerically solving equations 2 and 3. In Figure 2-a, a dashed curve corresponds to p(x,t) derived analytically as follows and dashed curves in Figure 2-b are obtained with equation 6. The fit between the numerical and semi-analytical values seems rather good.

Suppose that

$$f_s(v,x,t) \simeq \begin{cases} p(x,t), & v_0 \lesssim v \lesssim u(x,t) \\ 0, & v<v_0 \text{ and } v \gtrsim u(x,t) \end{cases} \qquad (5)$$

and the plateau $p(x,t)$ and $u(x,t)$ are known functions, we have after the integration of equation 3 with respect to v from v_0 to v,

$$\frac{\partial w}{\partial t} = \frac{mv^3}{2\pi\nu_p}(v-v_0)\left\{\frac{\partial p}{\partial t} + \frac{v+v_0}{2}\frac{\partial p}{x}\right\} - \frac{mv^4\nu_s}{2\pi\nu_p}p - \nu_c w + Sc \quad . \qquad (6)$$

This equation is useful for the direct application to the plasma waves excited by solar electrons producing type III bursts. Where, $p(x,t)$ is obtained analytically in the following way.

If ν_s and ν_c are zero, $p(x,t)$ is given after Ryutov and Sagdeev (1970) as a function of $f_s(0)$ given by equation 4. The effect of non zero ν_s and ν_c on p at x>>(scale heights for ν_s and ν_c) can be estimated by equation 3 after the integration with respect to t and x (Takakura, 1976). It is shown that this effect is equivalent to give $f_s(0)$ a lower velocity cut-off due to the collision losses.

References

Ryutov, D. D., and Sagdeev, R. Z. : 1970, Soviet Phys. JETP., 31, 39

Takakura, T. and Shibahashi, H. : 1976, Solar Physics, in press.

Takakura, T. : 1976, Solar Physics, submitted.

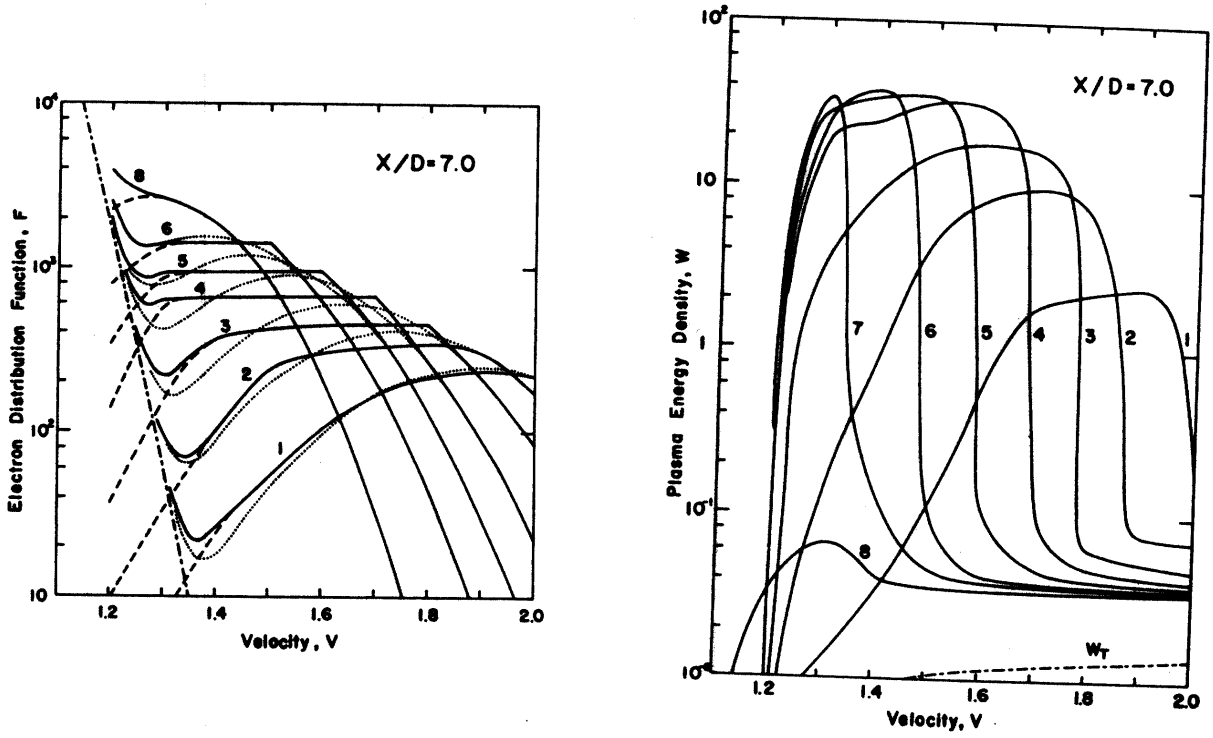

(a) (b)

Fig. 1. Dimensionless values of f and w are plotted against dimensionless velocity $V=v/v_0$, $v_0=2\cdot10^9$ cm/s. Serial numbers on the curves indicate a time series (time interval is not uniform). $N_0=4\times10^9$ cm^{-2}, $d=10^9$ cm, $\nu_p=100$ MHz, $\nu_c=\nu_s=Sc=0$.

(a) Dot-dashed curve; thermal electrons F_T. Dashed curve; beam electrons F_s. Solid curve; $F=F_s+F_T$. Dotted curve; F_s in free space i.e. free propagation where the interaction with the plasma is negligible.

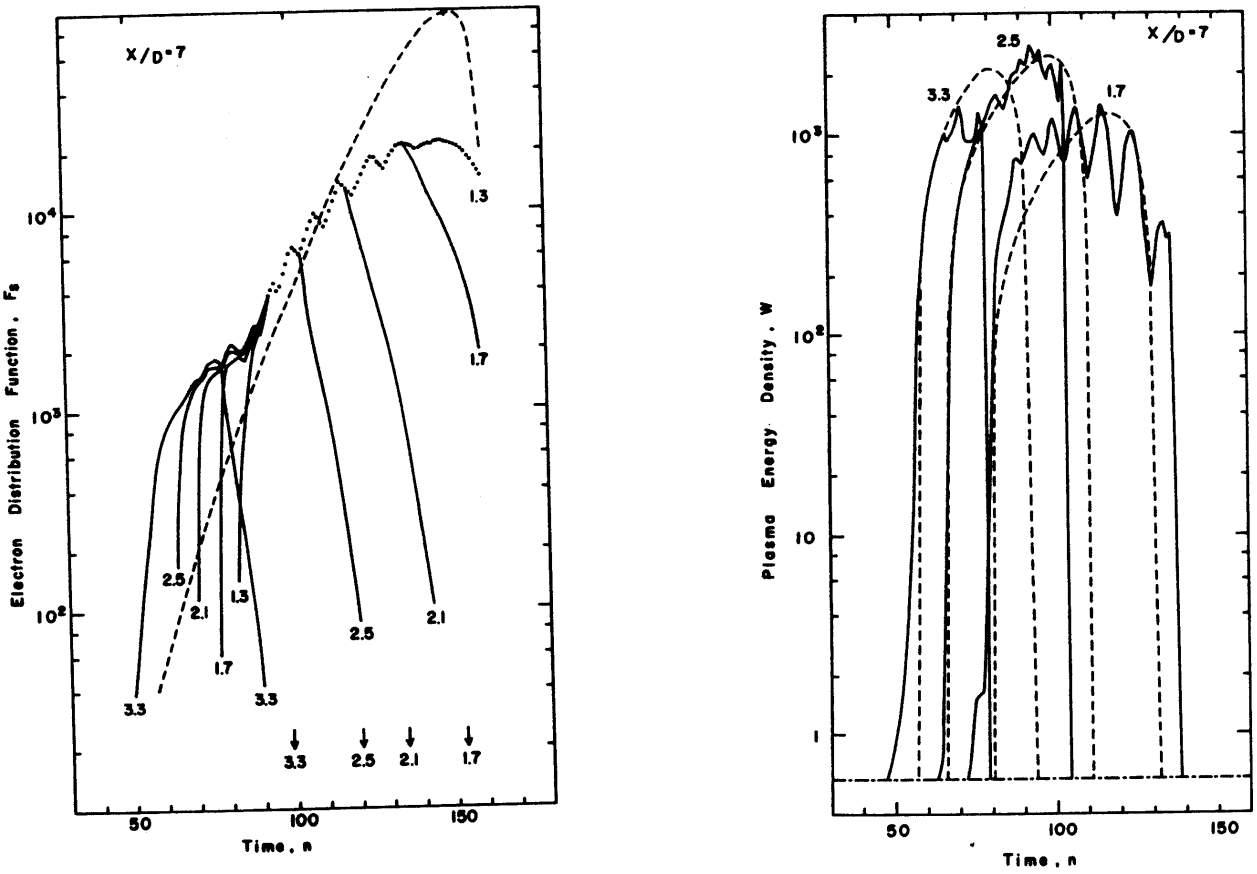

(a) (b)

Fig. 2. F_s and W are plotted against time (n=T/ΔT). Numerals on the curves indicate V. $N_0=10^{12}$ cm^{-2}, d=5·10^9 cm, Sc=0. Irregular oscillation of the dotted and solid curves are due to a finite width of mesh in the computation so that they are meaningless.

Experimental Studies on Beam–Plasma Interaction

Y.Kiwamoto

Research Institute for Energy Materials,

Yokohama National University

§1. Introduction

It is commonly accepted that electromagnetic radiations associated with solar flares, various perturbations in the geomagnetic field and so called aurora flares have relations with beams of electrons and/or protons ejected from the sun. The kinetic energy of the solar particles are transferred to the earth very effectively because the highly extended geomagnetosphere increases the interaction cross-section of the earth with the particles by far above that with photons. Properties of particle beams are frequently invoked in order to explain energetic phenomena observed in the magnetosphere and the ionosphere. However, it is well-known among experimenters of laboratory plasmas that the particle beams induce complex phenomena which are not easily explained. The nonlinear phenomena observed in the beam–plasma interaction are often beyond the theoretical prediction.

Recently technology of beam–handling has attained a level where highly controlled experiments of beam–plasma interaction are possible. I believe that various hypotheses and suppositions about the beam propagation and interactions in the space plasma can be proved or sometimes may be corrected by examining the specific processes in laboratory plasmas, which in turn will stimulate the activities of laboratory experiments.

In this article I would like to present briefly some results of my recent experiments. Details of these experiments are to be referred to papers published elsewhere.

§2. Ion Beam Instabilities in Unmagnetized Plasma[1)]

Ion-acoustic waves are spontaneously excited if an ion beam with velocity of the order of ion-acoustic velocity $c_s=(T_e/m_i)^{1/2}$ is injected either into an unmagnetized plasma or into a magnetized plasma in the direction of the magnetic field. Theoretical stability analysis has been proved in experiment. When the energy density of the beam is comparable with the thermal energy density of the background palsma, an ion= acoustic wave turbulence develops with energy density smaller by an order of 2 or 3. Three dimensional analyses of the turbulent waves have been made. The beam distribution relaxes so rapidly that they cannot be expalined by the binary coulomb collisions. Strong wave-particle interactions proposed by Dupree[2)] can explain the experimental results pretty well. A possibility of the formation of turbulent shocks[3)] has been discussed with negative conclusion.

§3. Ion Beam Instabilities Perpendicular to Magnetic Field[4)]

One of the characteristic modes which propagate at right angles to the magnetic field is the lower hybrid wave with frefrequency $\omega_{LH}=\omega_{pi}/[1+(\omega_{pe}/\omega_{ce})^2]^{1/2}$. Oscillations of this frequency have been observed frequently in rocket experiments. This mode grows with very large growth rate $[\gamma/\omega_r\sim 0.2]$ if an ion beam propagates at right angles to the magnetic field. The lower

hybrid instability is stronger as the beam velocity is increased in contrast to the ion-acoustic instability. Then high-temperature ions could be generated in this instability. Recently experimental studies of the instability have been made independently by R.P.HChang[5] and Y.Kiwamoto, M.Inutake and Y.Kita[4]. Stabilizing effect of the magnetic field should be taken into account in considering the evolution of the instability.

§4. Electron Beam Instability[6]

Various kinds of nonlinear phenomena have been observed in experiments on electron beam–plasma interaction. One of the current topics in this field is the plasma wave cavity formation due to the radiation pressure of spontaneously excited electron waves. The amplitudes of electron waves are bunched and trapped in density depressions executing the ion-acoustic motion. If such a phenomenon occurs in the space plasma, burts of electromagnetic radiation with frequency nf_{pe} (n:integer) may be observed correlated with burts of energetic protons. A.Y.Wong et al.[7] first reported this phenomenon then H.Ikezi et al.[8] made more extensive study with somewhat different conclusion. Y.Kiwamoto et al.[6] observed trapping of the electron waves in unstable ion-acoustic waves and relaxation oscillations between the two waves.

References

1) Y.Kiwamoto, J.Phys. Soc. Japan 37 (1974) 466.

2) T.H.Dupree, Phys. of Fluids 9 (1966) 1773.

3) D.A.Tidman, Phys. of Fluids 10 (1967) 547.

4) Y.Kiwamoto, M.Inutake and Y.Kita, IPPJ–

5) R.P.H.Chang, Phys. Rev. Letters 35 (1975) 285.

6) Y.Kiwamoto, H.Kuwahara and H.Tanaca, submitted for publication to J. Phys. Soc. Japan.

7) A.Y.Wong and B.H.Quan, Phys. Rev. Letters 34 (1975) 1499.

8) H.Ikezi, R.P.H.Chang and R.A.Stern, Phys. Rev. Letters 36 (1976)

Turbulent Plasma Phenomena in Space and Laboratory

Takaya Kawabe

Institute of Physics, The University of Tsukuba
Sakura-mura, Niiharigun, Ibaraki-ken 300-31, Japan
and
Institute of Plasma Physics, Nagoya University
Chikusa-ku, Nagoya 464, Japan

Abstract

Energy distributions of electrons and ions in turbulent plasmas are compared among the results from laboratory experiments, from computer simulation, and from sattelite measurement of earth's bow shock. Interaction of energetic ion beam with the turbulent plasma is discussed.

For the fusion between the laboratory experiments and the space plasma experiments, phenomena in turbulent plasmas have been considered in both the experiment as well as the results from computer simulations. Becuase of limitation of time and space for the meeting; only the distributions of the energy of the electrons and ions have been compared here.

Laboratory experiments on the turbulent plasma have been done as "turbulent heating of plasmas to achieve fusion temperature. Typical experimental arrangement (THE MACH II) is given in Reference 1. The parameters of the plasma are as follows: plasma density n: $10^{12} \sim 10^{14}/cm^3$ (hydrogen or helium) plasma temperature before heating discharge: 10 cV, for both electrons and ions, after discharge electron temperature 10 keV, ion temperature: a few keV heating discharge current: several 10 keV. The electron velocity distribution has been measured by use of Thomson scattering of ruby laser light,[1] while the ion energy distributions were obtained by optical measurements of Doppler broadeneing[2] and charge exchange neutral measurement.[3]

Measurements on velocity distributions of electrons and ions in turbulent plasmas of the earth's bow shock have been carried out with the Vela 4B electrostatic analyzer.[4] The computer simulations on the shock have been done by many authors, however, the results by C.T.Dum et al. was taking into account in this letter, for it seemed to present similar results with those of experimental.

The electron heating is observed to occurs earlier than

the ion heating in THE MACH II and bow shock. The energy distributions of the electrons in turbulent heating experiment show a flat-top shape at a certain time after the heating discharge started and when the ion acoustic instabilities grew up. The shape of the flat-top distribution has been observed in the space plasma when the sattelite enter the bow shock and also in the computer simulations by Dum et al. The formation of the flat-top could be interpreted by the quasilinear diffusion in velocity space when the ion acoustic turbulence existed, for the diffusion coefficient in velocity space contained a term of $(1/v_{\perp})$ where $v_{\perp}$ was perpendicular velocity to the direction of the current and it brought large diffusion in velocity space at lower velocity to give flat-top. In both laboratory experiment and space measurement show a slight concaveness of the space at some time and this cannot be explained by the quasilinear diffusion.

The ion energy distribution measured by charge exchange fast neutrals showed when the plasma become very resistive due to ion acoustic turbulence, an ion beam appeared on the tail of the distribution and it was smoothed within 1μ sec. This was explained as follows[5]: the high level of turbulence makes plasma very resistive and forms a large electric field through the plasma or shock like field so that the ions are accelerated to form an ion beam; and then the ion beam is thermalized by the ion acoustic turbulent waves. The theoretical calculation gave a good agreement with the experimental value. In the measurement at bow shock, the primary ion

beam came as the solar wind with a velocity of 400 Km/sec, and weak beam was also observed at 900 Km/sec. When the beam comes into the turbulent plasma in the shock, the energy spectrum becomes rather smoothed. This result might be explained[6] by the theory based on the model mensioned above. More refined experiments on the scattering of the ion beam by turbulent fluctuations in the plasma have been done[7)8)], and they were also interpreted as a random weak in the velocity space due to the turbulent electric field.[9)]

In conclusion, the comparison among the laboratory experiments, space measurements and computer simulations on the energy distribution of the electrons and ions in the turbulent plasmas gave similarity, which indicates that the mechamisms of heating of the electrons and ions in the turbulent plasmas are common among them.

1) K.Adati, H.Iguchi, Y.Ito, T.Kawabe, K.Kondo, O.Mitarai K.Muraoka and R.Sugihara: Phys. Rev. Letters 35 (1975) 280.

2) K.Adati, H.Iguchi, Y.Ito, K.Kawasaki, T.Oda, R.Sugihara T.Yokota: VII th European Conf. on Controlled Fusion and Plasma Physics, Lausanne, Swiss (1975).

3) Y.Nakagawa, et al. Proc. Vth International Conference on Plasma Physics and Controlled Nuclear Fusion, Tokyo Japan 1974 (IAEA, Vienna, Austria 1975) Paper C3-3.

4) M. D. Montgomery, J.R.Asbridge and S.J.Bame J. Geophysical Res., Space Phys, 75 1217 (1970).

5) T.Kawamura and T.Kawabe, 3rd International Conference on Theoretical and Experimental Aspects on Toroidal Plasma, Grenoble, France (1976), also Nagoya University Report, IPPJ-255 (1976).

6) T.Kawabe and T.Kawamura, to be published.

7) K,Ishii et al. in Ref.2

8) K.Yatsu, K.Nozaki et al. to be published.

9) S.Kojima and T.Kawabe: "Kakuyugo Kenkyu" Vol.35, Suppl.3 p.131 (1976).

Use of Fast Ion Beams in Plasma Research

Hiroshi Ishizuka

Institute of Physics, University of Tsukuba

1. Introduction

A plasma penetrated by an ion beam is a general configuration in space and in wide ranges of laboratory devices. In space physics, it has been hypothesized that the ion beam instability may play a role in the collisionless heating of the solar wind ions. From the viewpoint of basic plasma physics, an ion beam-plasma system offers a typical example of resonant wave-particle interaction. There have been a vast amount of theoretical and experimental works, and various aspects of instabilities driven by slow ions ($\lesssim$ tens of eV) have been clarified. Several kinds of waves have also been observed in magnetoplasmas penetrated by fast ions.

At the same time, interest in the ion beam-plasma interaction is closely connected to the use of ion beam in many fields of fusion research; neutral injection heating, two energy component system, build-up or start-up of mirror plasma, ion ring for field reversal, pellet implosion, etc. Up to now, however, there is no evidence that microinstabilities are excited by the injection of neutral beams into the plasma.

In this note, an outline of recent advances in ion beam technology is given, and it is pointed out that an ion (or neutral) beam has significant advantage over electron beams. Possible uses of intense beams will be discussed: creation of ion layer in a mirror field and formation of dense plasmas in the ionosphere, where the flight of a space shuttle is being scheduled.

2. Production of intense ion beams

Recently the development of ion source has been accelerated by the need in the field of fusion research. Quasi-steady generation of 14 keV 300 A neutral beam has been performed in 2XIIB experiment. The current density of 0.5 A/cm^2 and the power efficiency in excess of 60 % have been achieved. An injection system designed at Livermore for a future mirror reactor aims at 550 keV 550 A beam generated with overall efficiency of about 90 %.

In spite of the fact that an ion source requires more expensive and cumbersome machinery than the electron source, it is not the essential factor that limits the beam parameters. Problems in obtaining intense beams are the availability of power, damage of electrodes due to large heat flux, etc. We may thus assume that the parameters of fast ion beam can compete with those of electron beam at high intensities.

This way of thinking applies more clearly to very intense, pulsed ion beams. Successful generation of 100 kA ion beam with 10-100 ns duration has been achieved in the energy range of 0.1 to 1 MeV. The working principle of this sort of ion source is the same at the REB source. A diode is energized by a high voltage pulse of a short duration. Electrons emitted from a cold cathode hit the anode to form a plasma layer around it. Ions are extracted from this "anode plasma" and are accelerated toward the cathode by the strong electric field in the diode region.

Since the electrons are much more movable than ions, efficient ion beam generation implies suppression of net

electron current flowing into the anode. This can be realized by either a) making the anode transparent for energetic electrons, or b) utilizing the pinching effect of space-charge neutralized electron flow, or c) applying an external magnetic field. By these means, just a minor modification of REB source leads to the generation of a very intense ion beam, the efficiency being a modest fraction of that for REB generation.

3. Propagation of intense ion beams

In injection experiments, ion beams are converted into neutral beams so as to traverse across the magnetic field. If simply the self field of ion beam should be eliminated for the purpose of suppressing the beam divergence, an electron emitter is provided outside the ion source. In case of intense pulsed ion beams, charge and current-neutralization take place automatically owing to the electrons those are dragged along by the ions from the source. Furthermore, if the beam is dense enough, a neutralized ion beam can flow across a magnetic field by setting up surface polarization charges. These constitute a characteristic feature of the transport of intense ion beams.

4. Creation of rotating ion layer in a magnetic trap

As an example of the use of fast ion beam in laboratory, let us consider an application of a pulsed ion diode to a mirror machine. The scheme of proposed experiment is as follows. A rotating ion beam moving along the mirror axis is formed either by a) injecting a hollow beam through a magnetic cusp or b) injecting a beam azimuthally at the mirror end.

A dense background plasma is assumed to exist to short circuit the polarization field of the neutralized ion beam and allow the cyclotron motion of the beam ions.

It should be remarked that the complete short circuiting does not occur; there remains a radial space charge field in the beam cross section to sustain the azimuthal reverse current carried by drifting electrons, as a response to the rapid rise of ion current. The radial electric field will accelerate plasma ions and heat them through collisional and other processes.

An axial retarding force will be exerted to the beam ions due to the diamagnetic nature of the beam. If this force is not large enough to trap the rotating beam inside the mirror, one may apply a gate technique at the mirror end. An ion layer will thus be created. Although the stability of the ion layer is problematical, experimental results on the strong electron ring at Cornell indicate good gross stability.

In a design study which is underway at the University of Tsukuba, the parameters are chosen as follows: ion energy= 500 keV, beam current = 25 kA, beam duration = 60 ns, plasma density = $10^{13}/cm^3$ and plasma volume = 10^5 cm^3. We estimate that the radial electric field of about 20 kV/cm will arise and heat the plasma ions to keV range.

The ion layer is far from field reversing in our case. Even then, such a layer will serve as a barrier against the penetration of neutral atoms into the main body of plasma.

5. Formation of dense plasma in space

To my knowledge, the space shuttle is scheduled to fly in an ambient atmosphere where the density of oxygen molecules is as high as $10^{10}/cm^3$ and the density of plasma is typically $10^5/cm^3$. An ejection of electron beam into such a medium leads to both the charge-up of the vehicle and the strong divergence of the beam by the self field. These things are out of problem in the case of charge neutralized ion beam.

The neutralized ion beam will behave as a streaming plasma whose density much exceeds that of the natural plasma; the ion density of the beam is $10^9/cm^3$ for a 1 keV 10 mA/cm^2 beam of protons, and $10^{13}/cm^3$ for a 100 keV 1 kA/cm^2 pulsed proton beam. The density decreases with increasing distance from the vehicle, due to the initial divergence of the beam and to collisions with neutrals. Therefore, a wide range of density ratios between the artificial and natural plasma can be covered. Near the vehicle, the ratio of the plasma pressure to the magnetic pressure can exceed unity, and the Alfvén velocity as low as 10^6 cm/s will be realized without difficulty. In the frame moving with the beam, the natural plasma flows as a weak stream. In such circumstances, we may expect many interesting phenomena. Also the production of plasma from ambient molecules by fast ions may modify the ionosphere locally.

In summary, intense ion beams have increasing applications to laboratory experimetns and fusion research, and possibly to the active experiemtns in space.

HEATING OF LABORATORY PLASMAS

Takaichi Kawamura

Institute of Plasma Physics

Nagoya University

Nagoya, 464

In the study of heating of laboratory plasmas it is important not only to clarify the heating mechanism, but also to discover the effective method by which we get the high temperature plasma with critical thermonuclear condition. The temperature to which we attain by heating is decided from the balance between the speed of thermalization of the kinetic energy injected outside and the loss speed of the thermal energy in the plasma. If we write the absorption rate of thermal energy as R_H, the temporal change of the plasma temperature is given by

$$\frac{d}{dt}(nT) \cong R_H - \frac{1}{\tau_E}(nT) \qquad (1)$$

where T is the temperature expressed by the energy unit and τ_E is the energy confinement time and n is the particle number density. Eq.(1) is considered to hold for the electron and the ion separately. If we take $r_H \simeq R_H/n$ as the heating rate per paticle, we have $T_{max} \simeq r_H \tau_E$ for the maximum temperature.

The heating rate per particle, r_H, is given by the product of the average kinetic energy ω, which a particle gains through a certain acceleration process, and the frequency ν_T, which gives the speed of thermalization (thermalization frequency), that is,

$$r_H \simeq w\ \nu_T \tag{2}$$

Here ν_T is defined by the inverse of the time in which the kinetic energy of a particle is converted into the random thermal energy.[1] We illustarate the meaning of Eq.(2) on the basis of the random walk theory. The heating rate is given by $r_H \simeq m\ D_v$ where D_v is the diffusion coefficient in velocity space. From the expression, $D_v \simeq <(\Delta v)^2>/\Delta t$, we have $r_H \simeq m<(\Delta v)^2>/\Delta t$. So we have $w \simeq m<(\Delta v)^2>$ and $\nu_T \simeq (\Delta t)^{-1}$, where Δv is the velocity increment of a particle due to the successive acceleration process and Δt is the time step of randomization of particle velocity. The thermalization (randomization) frequency ν_T agrees with the classical collision frequency when the randomization of particle velocity is due to the two particle collisions. However, in some cases ν_T is not always given by the classical collision frequency but is given by an enhanced value. We should find such a case of heating in the further heating of high temperature plasmas because the classical collision frequency decreases when the plasma temperature becomes higher.

When the thermalization is caused due to the Coulomb collision, ν_T is equal to the two body collision frequency. We call this case as *classical*. A typical example of the classical case is Ohmic heating. In this case we have $r_H^e \simeq \eta\ j^2$ for the heating rate where η is the classical resistivity and j is the current density. If we use the expressions, $\eta = m_e\ \nu_{ei}/ne^2$ and $j = nev_D$ (v_D is the drift velocity of the electron), we have

$$r_H^e \simeq m_e\ v_D^2\ \ \nu_{ei} \tag{3}$$

for the electron heating rate of Ohmic heating, where ν_{ei} is the

electron-ion collision frequency. From the same physical consideration we have for the neutral particle injection heating as

$$r_H^{\,i} \simeq \frac{n_b}{n_i + n_b}\ \varepsilon_b\ \nu_{bi} \tag{4}$$

where ε_b is the energy of the ion-beam resulting from the ionization of the neutral beam and n_b and n_i are the beam number density and the plasma ion density respectively, and ν_{bi} is the collision frequency between the beam ion and plasma ion.

At the plasma heating in the inhomogeneous magnetic field of confinement the thermalization frequency has more enhanced value than the classical collision frequency because of the orbital motion of the particle in the complex magnetic field. We call this case as *neoclassical*. One of the remarkable cases is TTMP (transit time magnetic pumping) in which the ions trapped in the magnetic mirrors of the pumping field make a substantial contribution to heating [2]. In this case the potential energy $\mu\tilde{B}$ of the trapped particle in the wave field is thermalized when this particle is detrapped by collisions and the frequency of detrapping is larger than the collision frequency because of the smallness of the mirror ratio of the magnetic wave field. Another example is the stochastic heating in ECRH (electron cyclotron resonance heating) in a magnetic mirror device [3]. In this case electrons are accelerated coherently in the ECR regions produced in the mirror by rf power and outside these regions they move almost adiabatically. When the relations between the phases of the electron gyration and electric field oscillation at the entry in the resonance region is random, the electorn does random walk in $v_\perp$-space in the course of bouncing motion in the magnetic mirror and the heating results. In this case ν_T is always given by the inverse of the recurrence

time to the resonance region in so far as the gyration phase is randomized in the bouncing motion.

Finally we refer to the case which should be called as the *turbulent* case. In a quiescent plasma the collision frequency of the electron with ions is expressed as

$$\nu_c^e \simeq \omega_{pe} \frac{1}{n \lambda_D^3} \tag{5}$$

without a numeriacl factor of the order of unity, where ω_{pe} is the electron plasma frequency and λ_D is the electron Debye length. When the plasma becomes turbulent and the fluctuation level becomes larger than that in the thermal equilibrium, the relaxation of the motions of electrons turns out to be subject to the scattering by the turbulent wave field. Then, the effective collision frequency ν^e_{eff}, which determines the electric resistivity and the heating rate of electrons, is given by the similar equation to (5), which has an another factor in place of $(n\lambda_D^3)^{-1}$. For example, using the quasilinear theory and some assumptions we have[1]

$$\nu^e_{eff}(v) \cong \omega_{pe} \frac{W}{nTe} \cdot \frac{\lambda_D}{\lambda_c} \left(\frac{v_{Te}}{v}\right)^3 , \tag{6}$$

where W is the electrostatic field energy of the turbulent wave, λ_c is the characteristic wave length (correlation length) of turbulent waves and v_{Te} is the thermal velocity of the electron. In general we may express the effective collision frequency of the electron due to the turbulent wave as

$$\nu^e_{eff} \sim \omega_{pe} \frac{W}{nT_e} \tag{7}$$

without a numerical factor depending on the model of turbulence. Then we obtain the heating rate of anomalous Ohmic process as

$$r_H^e \simeq m_e v_D^2 \nu_{eff}^e \quad . \tag{8}$$

As to the ion heating, this anomalous relaxation process also works effectively. The effective collision frequency of the ion due to the turbulent wave becomes

$$\nu_{eff}^i(v) \simeq \omega \frac{W}{nT_e} \frac{m_i}{m_e} \left(\frac{v_{Te}}{v}\right)^2 \quad , \tag{9}$$

where ω is the characteristic frequency of the turbulent field and is of the order of ω_{pi} in the case of the ion acoustic turbulence which is considered to be effective to the ion heating. If there exists a process which produces energetic ions, for example, a potential cliff which accelerates a portion of plasma ions, the enhanced fluctuation in the turbulent plasma always promotes the thermalization of such ions and this effect should be considered as the most important in the further heating of a high temperature plasma in which the classical collision frequency inevitably becomes small.

REFERENCE

[1] T. Kawamura and T. Kawabe; Research Report, Institute of Plasma Physics, Nagoya Univ. IPPJ-255, and *Conf. Proc. on Experimental and Theoretical Aspects of Toroidal Plasmas*, (Grenoble) Vol.2 p179 (1976).

[2] E. Canobbio; Sym. Plasma Heating and Injection, Valenna 1972 Editorice Compositori, Bologna p.14 (1973)

[3] T. Kawamura, H. Momota, C. Namba and Y. Terashima; Nuclear Fusion 11, 339 (1971)

LABORATORY AND SPACE EXPERIMENTS ON BEAM - PLASMA INTERACTION

N. Kawashima

Institute of Space and Aeronautical Science
University of Tokyo
(Komaba, Tokyo 153)

A number of experiments have been performed in laboratories to study the physics of beam-plasma interaction. They started in the linear dispersion regime and now people are interested in non-linear and turbulent regime. Especially, the recent trend is to used high power electron beams related in thermonuclear fusion research.

A relativistic high intensity electron beam (REB) is one of them. REB is interesting in a sense that the current is high enough so that the magnetic energy of the beam becomes important.

Topics of the beam-plasma interaction are :

i) Strong plasma heating by the beam-plasma interaciton, especially the importance of the existence of the reverse current.

ii) Strong electromagnetic radiation generated in the beam-plasma interaction.

iii) Neutron production in the plasma heating.

We have been doing a beam-plasma interaction experiment using a 500 keV, 2 kA, 3 nsec electron gun. This electron beam source has not a large stored energy compared with other multi-hundred kilo joule experiment, but the pulse width is very short (More than an order of magnitude less). Fig. 1 shows an experimental layout of the experiment. A plasma is produced by a plasma gun and injected in the magnetic field. In this experiment, we have obtained the following results :[1], [2], [3]

i) The existence of the reverse current and magnetic shielding effect. (Fig. 2)

ii) A strong plasma heating (Fig. 3)

iii) An electromagnetic radiation that lasts after the end of the beam pulse in the vicinity of cyclotron harmonics. (Fig. 4)

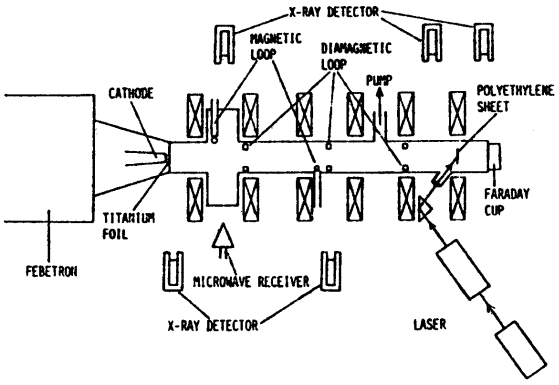

FIG. 1. Schematic view of the experimental setup.

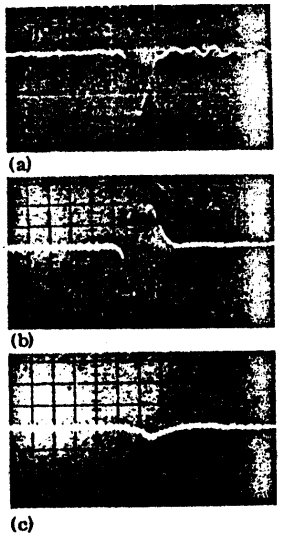

FIG. 2. Oscilloscope traces of relativistic electron beam. (a) Current measured by Faraday cup: 10 ns/div. (b) Time derivative of the magnetic field produced by the relativistic electron beam in vacuum; 5 ns/div. (c) Time derivative of the magnetic field in the plasma; 5 ns/div.

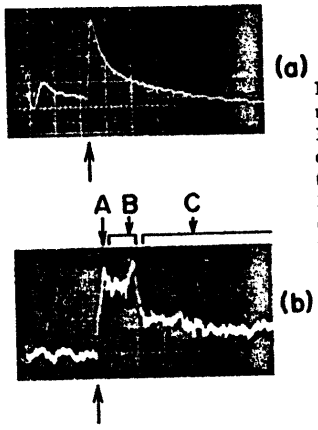

FIG. 3. (a) Diamagnetic signal measuring nkT of plasma; 12.5 μs/div. (b) Microwave emission from the plasma at the second cyclotron harmonic: 10 μs/div. Three types of emissions, A, B, and C, are indicated. The time of beam injection is shown by arrows.

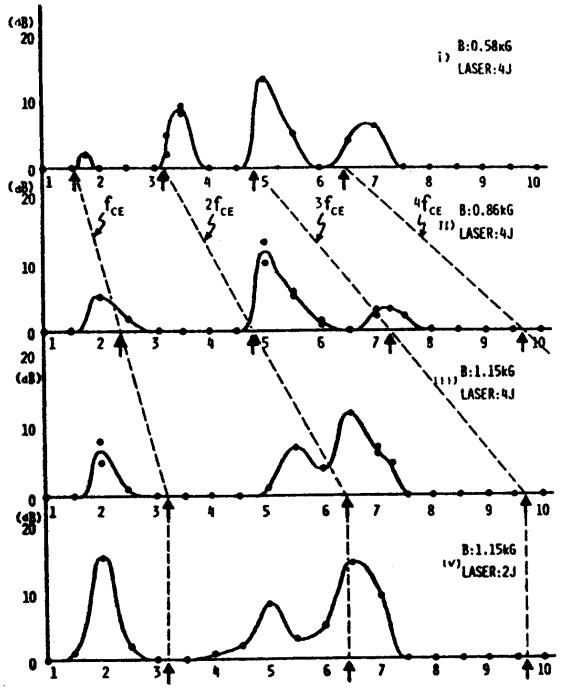

FIG. 4. Frequency spectra of the long-lasting microwave emissions (emission C); B is the external magnetic field strength and LASER means the laser energy for the production of the plasma. Electron cyclotron harmonics are denoted by arrows in each spectrum.

The beam-plasma interaction is also very important is space physics. A member of phenomena can be found in which the electron beam should play an important role. For example, the generation of VLF waves in the earth's magnetosphere, the Type III bursts of the electromagnetic radiation in solar flares, etc. So far these research have beam based on passive observations. The development of spacecrafts such as rockets and satellites has contributed enormously to obtain a large amount of natural data and to study the physical mechanism of the phenomenon. However, natural phenomena are so complex that there still remain a considerable amount of problems unsolved and most of them are substantial to understand the physical mechanism. A recent development in space experiments is an active (controlled) experiments.

It means to perturb the nature by an active means and to control natural phenomena. Most typical ones are

i) Electron beam ejection

ii) Production of artificial Ba plasma clouds (Chemical release)

iii) Emission of high power RF waves

Some of them have been successfully performed by rocket experiments. These experiments, however, requires a large weight and size of payloads and a long experiment time.

Rockets and satellites cannot satisfy these requirement.

The most possible way is to use Space Shuttle which will be used from the beginning of 1980's. The first flight of Spacelab (Laboratory on the Space Shuttle now developed by ESA (European Space Agency)) is scheduled in autumn 1980. The anouncement of opportunity was issued in this spring and we (T. Obayashi, N. Kawashima, K. Kuriki, M. Nagatomo

and I. Kudo) have proposed an electron and plasma beam experiment called SEPAC (Space Experiments with Particle ACcelerators). The major feature of the proposal is as follows and a new era of space plasma experiments will come soon.

The main scientific objectives of the experiments are:

1) Vehicle Charge Neutralization

2) Beam Stability and Beam-Plasma Interactions

3) Beam-Atmosphere Interactions

4) Feasibility Studies for Measurements of E and B Field Morphology

5) Modification of Ionosphere Parameters

The SEPAC-MINI System consists of the following subsystems:

i) Electron Beam Accelerator (EBA)

Voltage	1-20 kV (Gun Options: 50 kW, 25 kW, 10 kW)
Current	2.5 A max
Pulse-width	10 ms - 1 sec variable
Modulation	10-100 Hz, 100 kHz - 10 MHz
Beam Deflection with Focusing	XY, XZ plane ± 30°

ii) Magneto Plasma Dynamic Arcjet (MPD-AJ)

Energy Input	10 kJ/pulse max (Gun: 2-5 kJ unit)
Ion-pairs Number	10^{20}/pulse
Voltage	250 V
Pulse-width	2 ms
Gas	He, A, N_2

iii) Monitor and Diagnostic Equipment

iv) Control, Display and Data Management

The associated diagnostic instruments include beam-monitor TV imagers, wave and particle measuring instruments, retarding potential analyzers and other plasma probes. Throw-away detectors with wave-particle diagnostic packages and ground-based/aircraft observations are desirable to support the experiment, if they are available.

Experiment operations are performed in the Shuttle orbit. Since the present experiment cannot be made without a close coordination in space and the ground network, payload specialists must control the mode of instrument operation based on a real-time evaluation of conditions encountered. He may also be able to participate in many other real-time operational functions, such as the accelerator handling, photographing the luminous clouds, etc..

SEPAC ACCELERATOR SYSTEM*

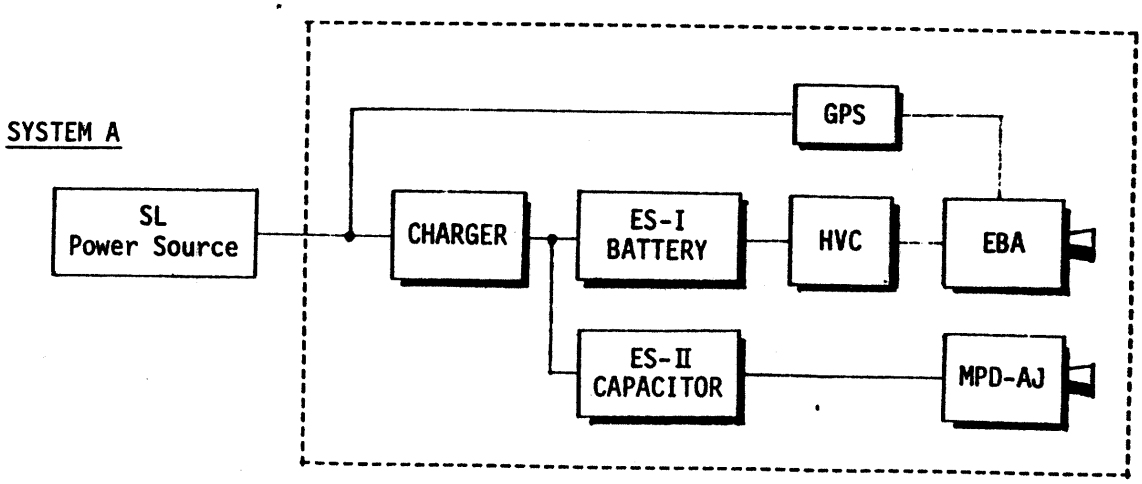

REFERENCES

1) R. Okamura and N. Kawashima, Physics Letters 54, 101 (1975)

2) R. Okamura, Y. Nakamura and N. Kawashima, Applied Physics Letters 28, 701 (1976)

3) R. Okamura, Y. Nakamura and N. Kawashima, ISAS Research Note 21 (1976)